VISUAL MOTION PERCEPTION
AFOSR Final Technical Report
(F49620-97-1-0028)

by

Kathleen A. Turano

The Johns Hopkins University School of Medicine
Wilmer Eye Institute
550 N. Broadway, 6th floor
Baltimore, Maryland 21205
Voice: (410) 502-6434
FAX: (410) 955-1829
Email: kathy@lions.med.jhu.edu

March 6, 2000

AFRL-SR-BL-TR-00-

0075

REPORT DOCUMENTATION PAGE

1. AGENCY USE ONLY (Leave Blank)	2. REPORT DATE	3. REPORT TYPE AND D ... COVERED
	6 Mar 2000	15 Mar 97 - 14 Dec 98 FINAL

4. TITLE AND SUBTITLE

Visual Motion Perception

5. FUNDING NUMBERS

Grant No:
AFOSR-F49620-97-1-0028

6. AUTHORS

Kathleen A. Turano

7. PERFORMING ORGANIZATION NAME(S) AND ADDRESS(ES)

Johns Hopkins University School of Medicine
Wilmer Eye Institute
720 Rutland Avenue
Baltimore, MD 21205

8. PERFORMING ORGANIZATION REPORT NUMBER

52-0595110

9. SPONSORING / MONITORING AGENCY NAME(S) AND ADDRESS(ES)

AFOSR/NL
Building 410
Bolling AFB, D.C. 20332-6448

10. SPONSORING / MONITORING AGENCY REPORT NUMBER

AFOSR's CFDA
#12,800

11. SUPPLEMENTARY NOTES

12a. DISTRIBUTION / AVAILABILITY STATEMENT

DISTRIBUTION STATEMENT A
Approved for Public Release
Distribution Unlimited

12b. DISTRIBUTION CODE

13. ABSTRACT *(Maximum 200 words)*

In operations of aircraft control or target acquisition, the misperception of motion could produce serious errors in a pilot's performance. Little is known about the human observer's ability to accurately judge the velocity of motion while navigating through an environment containing moving objects or while making eye movements. If we can understand how the perception of motion is affected by the presence of moving objects in the environment or by eye movements, we can then specify viewing requirements based on the perceptual cost/benefits. In this project, the human observer's ability to judge velocity was investigated in two sets of experiments. In the first set of experiments the ability to judge self motion in an environment containing moving objects was investigated using simulated optic flow displays. The effects of object and observer velocity on the ability to discriminate between curvilinear and rectilinear self motion were determined. In the second set of experiments, the ability to judge object velocity while making smooth pursuit eye movements was investigated. The effects of stimulus velocity, size, and eccentricity on velocity perception were determined. The findings from the eye-movement experiments led to the development of a model that explains how eye velocity signals combine with visual motion signals to determine the perception of motion.

14. SUBJECT TERMS	15. NUMBER OF PAGES
egomotion, motion perception, curvilinear motion, self motion perception, pursuit eye movements	34
	16. PRICE CODE

17. SECURITY CLASSIFICATION OF REPORT	18. SECURITY CLASSIFICATION OF THIS PAGE	19. SECURITY CLASSIFICATION OF ABSTRACT	20. LIMITATION OF ABSTRACT
Unclassified	Unclassified	Unclassified	Unlimited

TABLE OF CONTENTS

LIST OF FIGURES

CHAPTER I

INTRODUCTION

In operations of aircraft control or target acquisition, the misperception of direction and/or speed of motion could produce serious errors in the pilot's performance. Little is known about the human observer's ability to accurately judge the direction and/or speed of motion as he or she navigates through an environment containing moving objects or while making smooth pursuit eye movements. If we can understand how the perception of motion is affected by the presence of moving objects in the environment or by eye movements, we can then specify viewing requirements based on the perceptual cost/benefits.

In this report we describe the findings of several studies. In the first set of experiments, we investigated the human observer's ability to judge self motion using optic flow displays that simulate movement through an environment containing moving objects. In this set of experiments we specifically examined the effects of object speed and direction on the discrimination of curvilinear and rectilinear self motion. In the second set of experiments, we investigated the effect of eye movements on motion perception. We specifically examined the effects of stimulus velocity, size, and eccentricity. In addition, we describe a model that we developed to explain how eye velocity contributes to motion perception.

CHAPTER II

DISCRIMINATION OF SELF-MOTION PATHS IN ENVIRONMENTS CONTAINING MOVING OBJECTS

As we move within our environment the movement of our body produces a change in the pattern of light intensities projected to our retinaes. This change, called optic flow,(Gibson, 1950) indicates the direction of body movement relative to the environment and can be used to guide locomotion. Optic flow can be represented as a velocity field where each vector depicts the optical speed and direction of an environmental element at that location. When a person moves forward along a straight path through a stationary environment, the optic flow that is generated is a radial expansion pattern, and the person's heading direction is specified by the flow vectors' common point of origin, called the focus of expansion (FOE). If a person looks straight ahead and makes no eye movements, the structure of the optic flow is radial in his/her central visual field and lamellar in the periphery. Human observers can use computer generated patterns of optic flow to accurately judge the simulated heading direction along a straight motion path(Warren & Hannon, 1988; Warren, Morris, & Kalish, 1988) and also to accurately judge the direction of a change in heading direction.(Riemersma, 1981; Turano & Wang, 1994)

When the environment contains an independently moving object, the structure of the optic flow in the area of the moving object is altered. When the object translates in depth, a secondary focus of expansion, FOE´, is generated. When the object translates along the fronto-parallel plane, a local region of parallel flow is generated in the area of the moving object. Thus, when the environment contains a moving object, the motion vectors no longer have a common point of origin (unless the object approaches the observer on a parallel path).

The presence of a moving object has been shown to affect the perception of heading direction.(Cutting, Vishton, & Braren, 1995; Royden & Hildreth, 1996; Warren & Saunders, 1995a; Warren & Saunders, 1995b) Heading-direction bias is dependent upon the direction of the object motion. Object motion that consists predominately of lateral motion produces a bias in the direction of the object motion whereas object motion that consists of a large expansion component produces a bias in a direction away from the object motion. These studies showed small effects

even for large moving objects, but they failed to manipulate object speed to determine whether the speed of the moving object had an effect on the perception of self motion.

In this set of experiments we explored how the velocity (both speed and direction) of a moving object affects an observer's ability to use the optic flow pattern to determine his or her path of self motion. We used a temporal two-alternative, forced-choice staircase procedure, without feedback, to determine the threshold angular speed (i.e. the minimum deviation from a straight path) required to discriminate curvilinear from rectilinear simulated self motion. In some blocks a simulated moving object was present, in others there was no object. In Experiment 1, the object consisted of a collection of dots that moved together in depth (toward and away from) relative to the observer (Figure 1). The initial position of the simulated object was 20 m from the observer. Observer and object velocities were manipulated.

Figure 1 about here

Figure 2 shows threshold angular speed plotted against the speed of an object moving in depth. The results show no consistent pattern. For some observer speeds, thresholds increased with increases in object speed. For other observer speeds, thresholds decreased. Also shown in the figure are the discrimination thresholds obtained with optic flow patterns void of moving objects (indicated on the x-axis as "No"). When the patterns contained no object, thresholds increased with observer speed. Discrimination thresholds were lowest for an observer speed of 15 m/sec and highest for an observer speed of 35 m/sec. This pattern of results is consistent with what we have reported previously. (Turano & Wang, 1994)

Figure 2 about here

The threshold values of Figure 2 are replotted against object speed relative to observer speed in Figure 3. Positive values of relative object speed represent objects moving faster than the observer and negative values represent objects moving slower. A relative object speed of 0 m/sec indicates that the object was moving at the same speed as the observer. Symbols differentiate observer speeds (closed circle: 15 m/sec; open squares 25 m/sec; solid diamonds 35 m/sec).

Figure 3 about here

The results show a systematic pattern when plotted against relative object speed. Subjects' ability to discriminate between a curvilinear and rectilinear self-motion path with optic flow patterns that contained a moving object decrease with increases in the speed difference between the object and the observer. Compared to patterns with an object that moves at the observer's speed, discrimination thresholds for patterns with an object that moves 20 m/sec faster or slower than the observer were1.5 to 2 times higher. The results showed that the critical factor in determining threshold angular speed for path discrimination is not the speed of the object, per se, but rather the speed of the object relative to the speed of the observer.

For the two highest observer speeds, 25 m/sec and 5 m/sec, thresholds were higher when the patterns contained no objects compared to when moving objects were present (for the relative object speeds that we tested). However, for the slowest observer speed,15 m/sec, thresholds obtained with patterns that contained no moving objects were comparable to those obtained when the object moved at the same speed as the observer.

Figure 4 illustrates the magnitude of the "benefit" for discriminating self-motion paths resulting from the presence of moving objects in the optic flow patterns. Benefit was calculated as the threshold obtained with the pattern containing no objects minus the threshold obtained with the pattern containing a moving object. In Figure 4 the magnitude of the benefit is plotted against the relative speed of an object moving in depth. The symbol notation is the same as in Figure 3. Positive values of benefit indicate that the subject was better able to discriminate between a curvilinear and rectilinear path when the optic flow pattern contained moving objects. Negative values indicate that the presence of a moving object hindered discrimination, and a benefit of 0 indicates that the presence of a moving object did not affect discrimination performance.

Figure 4 about here

The results showed that when an object moves in depth at a speed slower or equal to the speed of the observer, the presence of the moving object improves, or at the least does not affect, discrimination performance. But when an object moving in depth moves considerably faster than the observer its presence detrimentally affects discrimination performance.

CHAPTER III

EYE MOVEMENTS AND MOTION PERCEPTION

The goal of the next set of experiments was to investigate the human observer's ability to judge object (or stimulus) motion during smooth pursuit eye movements.

Effect of stimulus velocity

We investigated the relation between the perceived speed of a moving stimulus and eye velocity. We tested the hypothesis that smooth pursuit eye movements can affect the perceived speed of moving stimuli. We had subjects match the speed of a test stimulus, viewed while tracking a separately moving target, to the apparent speed of a reference stimulus, viewed with the eye stationary. Figure 5 shows the speed match thresholds for a stimulus reference speed of 2°/sec as a function of eye velocity. If the retinal image motion due to eye movements were fully compensated, we would expect the thresholds to fall on the dashed line indicating that, regardless of eye velocity, the stimulus velocities were perceived to be the same. If the retinal image motion due to eye movements were not compensated, we would expect the thresholds to fall on the solid line indicating that the retinal velocities of the stimuli were the same at a perceived match. If the retinal image motion due to eye movements were partially compensated, we would expect the thresholds to fall somewhere between the solid and dashed lines. The shaded area is the region predicted by traditional models of compensation, with extra-retinal gains ranging from 0.6 to 0.9. (de Graaf & Wertheim, 1988; Freeman & Banks, 1998; Mack & Herman, 1972)

Figure 5 about here

There are many interesting points to note about the results. One, the speed match thresholds did not all fall on the dashed line. This confirms the hypothesis that smooth pursuit eye movements can affect the perceived speed of moving stimuli. Two, the speed match thresholds did not all fall on the solid line, indicating that some degree of compensation occurs under some conditions. Three, the relative direction of the eye movement to the stimulus motion affects the degree to which eye

movements are compensated for motion perception. For example, an eye movement of 1.5°/s in the opposite direction of the stimulus produced a speed match error of less than 0.3 °/s. But a 1.5°/s eye movement in the same direction produced an error of greater than 1°/s. Four, the data are not well predicted by the traditional model of compensation. Some speed match thresholds fell outside the region predicted by the traditional model. The results of this study indicate the need to more fully explore the role of eye movements on motion perception and revise the model for compensation.

Effect of stimulus size or eccentricity

We tested the hypothesis that the size of a stimulus can affect its perceived speed during smooth pursuit eye movements. Using the same procedure as described above, we determined the speed of a test stimulus, viewed while tracking a separately moving target, to match the apparent speed of a reference stimulus, viewed with the eye stationary. Speed match thresholds were determined for two display sizes (8° x 8° and 38° x 28°). Figure 6 plots the speed-match thresholds.

Figure 6 about here

The most striking finding in the results is that a stimulus's characteristics can influence the effect of eye movements on the perceived velocity of the stimulus. There is a significant difference between the data for the large and small stimulus displays when the eyes move in the opposite direction to the stimulus. With the large display, eye movements decrease the perceived speed of the stimulus, and with the small display, eye movements increase the perceived speed of the stimulus. The size of the display was not a significant factor for perceived speed when the eyes moved in the same direction as the stimulus.

Because the size of the display was directly related to the eccentricity of the moving stimuli, it is possible that the critical factor for perceived speed was not stimulus size, but rather the part of the retina being stimulated. With the small display, the stimulus was confined to the central retina, whereas with the large display, the stimulus extended into the periphery. To separate the effects of size and eccentricity, we ran another experiment. We obtained speed match thresholds for a 2°/s

stimulus reference speed and a pursuit target speed of - 2 °/s using three different stimulus configurations. One configuration (Figure 7A) was similar to the small display. Another configuration (Figure 7B) was similar to the large display. The third configuration (Figure 7C) consisted of a stimulus that extended to the outermost peripheral region of the large display equating eccentricity but the central region was void of dots in order to equate stimulus size to the small display. If size is the critical factor, we would expect similar thresholds for configurations A and C. If eccentricity is the critical factor, we would expect similar thresholds for configurations B and C.

Figure 7 about here

The speed match thresholds for configurations B and C were similar: the mean thresholds for configurations A, B, and C were 1.4°/sec, 2.4°/sec, and 2.6°/sec, respectively. These results indicate that eccentricity, and not size per se, affects perceived velocity during eye movements.

Eye-movement compensation model for motion perception

Smooth pursuit eye movements add a velocity field to the visual scene, changing the speed and/or direction of the motion in the retinal image. Therefore, in order to recover the real-world motion, the velocity field added by the eye-movements must be discounted. The traditional view is that the visual system compensates for changes in the retinal-image motion caused by smooth pursuit eye movements by subtracting an extra-retinal signal, that carries information about those eye movements, from the signal reflecting retinal-image motion.(von Helmholtz, 1962; von Holst, 1954) According to this theory the perception of motion reflects the difference between these signals. However, studies have shown that for motion perception eye movements are not fully compensated. Human observers make perceptual errors in the speed and direction of moving objects when their eyes are moving.(Freeman & Banks, 1998; Turano & Heidenreich, 1999; Wertheim & Van Gelder, 1990) This lack of compensation has often been regarded as representing a less-than-unity gain for the eye-velocity signal. The modification of the traditional model states that perceived velocity is the

difference between the signals representing the retinal-image motion and eye velocity scaled by a gain factor.

Although this model can account for some findings, more recent studies(Freeman & Banks, 1998; Haarmeier & Thier, 1996; Turano & Heidenreich, 1999; Wertheim & Van Gelder, 1990) challenge this simple modification of the traditional theory. For example, the compensation of eye movements for motion perception has been shown to be influenced by the relative direction of the eye movement and stimulus motion,(Turano & Heidenreich, 1999; Wertheim & Van Gelder, 1990) preceding stimuli,(Haarmeier & Thier, 1996) and stimulus characteristics. Some of the stimulus characteristics that have been shown to affect the compensation are size,(Turano & Heidenreich, 1999; Wertheim & Van Gelder, 1990) retinal eccentricity,(Turano & Heidenreich, 1998) duration,(Ehrenstein, Mateef, & Hohnsbein, 1987) and spatial frequency.(Freeman & Banks, 1998) These studies indicate that the process by which the visual system compensates for changes in the retinal-image motion caused by smooth pursuit eye movements is not as simple as had been previously thought.

Freeman and Banks(Freeman & Banks, 1998) have recently proposed another linear model of perceived velocity that consists of an extra-retinal signal that inaccurately estimates eye velocity and a retinal-velocity signal that inaccurately estimates the retinal velocity. The inaccuracies can be viewed as gains (or weights) of the signals. In the Freeman and Banks study, the stimulus spatial frequency was shown to modify the perceived speed of the stimulus during eye movements. Their model, with a retinal-velocity signal gain that varied with stimulus spatial frequency and an extra-retinal signal gain that remained constant, could explain the data.

The aim of this study was to determine whether the visual system combines the retinal and extra-retinal signals in a linear manner to discount the added velocity field due to smooth pursuit eye movements for the perception of motion. To do so, we needed a method that would allow the determination of the separate contributions of the retinal-velocity signal and the extra-retinal signal for the perception of stimulus velocity. To this end, we developed a method to control the retinal

velocity in the presence of eye movements, i.e. the fixate-pursue procedure with controlled retinal velocity.

The retinal velocity of the object motion (referred to as the stimulus) is controlled by the stabilization of the stimulus display with a Generation V dual Purkinje image eye tracker (see Figure 8). The target for pursuit and fixation is presented on a separate monitor from the one that displays the stimulus, and the images on the two monitors are superimposed optically. With this method, the eye movements are monitored by the eyetracker and the signals are sent to the servo-controlled mirrors (designated in the figure as horizontal and vertical deflection mirrors) that rotate in response to the signals to compensate for the subject's eye movements. The images on the stimulus display pass through this optical path with the result that the retinal velocity of the moving stimulus is unaffected by eye movements. A half-silvered mirror is positioned at location A in order to produce another optical path in which stimuli presented on a separate display monitor could pass through, bypassing the optical path used for stabilization. We present a target that is used for pursuit and fixation on this second display with the result that its retinal image undergoes changes consistent with a person's eye movements.

Figure 8 about here

We used this method to test the hypothesis that an extra-retinal signal, which carries information about the smooth pursuit eye movements, combines in a nonlinear manner with retinal velocity to determine perceived velocity. To do so, we had subjects adjust the speed of a test stimulus, viewed with a stationary eye, to match the apparent speed of a reference stimulus, viewed during a pursuit eye movement.

On each trial, a moving stimulus (shown in Figure 9 as translating dots) was presented twice in succession. In the first presentation, the stimulus moved at a *test speed*, which is a pre-determined reference speed ± a delta speed. During this presentation, the subject fixated a stationary spot. In the second presentation, the stimulus moved at the reference speed, and the subject tracked the pursuit target (a spot translating across the screen). After each trial, the subject indicated whether the stimulus in the first presentation was faster or slower than the stimulus in the second presentation.

On the next trial, the *test speed* was decreased or increased depending on the subject's response on the previous trial. This process continued until the subject reported that the two speeds were equal. At the point of perceptual equivalence, the *test speed* defined the speed match threshold.

Figure 9 about here

We measured speed match thresholds for a reference speed of 0°/sec. As shown in Figure 10, and corroborated by the subjects' verbal comments, the stationary stimulus (0°/sec) was perceived to move in the same direction as the smooth pursuit eye movement. This illusory motion is the consequence of the compensation process. Because the retinal velocity of the stationary stimulus was 0°/sec, the speed match threshold reflects the retinal velocity equivalence of the extra-retinal signal. The data show that the magnitude of the speed match threshold increases with increasing eye velocity for both leftward (shown as negative eye velocity) and rightward (positive eye velocity) eye movements.

Figure 10 about here

The results of the previous experiment demonstrated that smooth pursuit eye movements generate an internal motion signal, i.e. an extra-retinal signal, that is in the same direction as the eye movement and is indistinguishable from a motion percept generated from retinal image motion. In this experiment we examined how the extra-retinal and retinal velocity signals combine. Velocity match thresholds were determined for reference speeds of 2°/s and 4°/s. The center and bottom rows of Figure 11 show the graphs of the velocity match thresholds for reference velocities of 2°/s and 4°/s, respectively. The three subjects' data are shown in separate columns. The retinal velocities of a test stimulus perceived to be equal to the reference stimulus viewed with moving eyes are plotted against eye velocity. Negative and positive values of eye velocity indicate eye movements in the opposite and same direction to the stimulus. As shown, the data appear to flatten out for eye movements in the same direction as the stimulus (positive values of eye velocity).

Figure 11 about here

Guided by the data in Figure 11 we developed a model to explain perceived velocity in the presence of smooth pursuit eye movements. The model was successful in explaining the data. The

model takes the difference between two simple saturating nonlinear functions, *g* and *f*, each symmetric about the origin, but one having an interaction term. That is, the function *g* has two arguments: retinal velocity, $\dot{R}$, and eye velocity, $\dot{E}$. Each argument has a scaling parameter. The function *g* is specified as

$$g[\dot{E},\dot{R}] = R'_{max}\left(\frac{1}{1+e^{-\varepsilon\dot{E}-\alpha\dot{R}}} - 0.5\right) \quad \text{Equation 1}$$

The only argument to *f* is retinal velocity, $\dot{R}$. The function *f* is specified as

$$f[\dot{R}] = R_{max}\left(\frac{1}{1+e^{-\rho\dot{R}}} - 0.5\right) \quad \text{Equation 2}$$

We determined the values for the four free parameters (ε, ρ, R_{max}/R'_{max}, and α) using a least squares fit to the combined dataset. The model fits are shown as solid lines in the rightmost graphs of Figure 12. As shown in the graphs, the model provides a good fit to the data of all three base velocities, despite the fact that the model was applied to the combined dataset.

A comparison of the goodness of fit between the nonlinear compensation model and traditional linear models (shown in the leftmost graphs) demonstrates that the nonlinear model better explains perceived velocity in the presence of smooth pursuit eye movements.

Figure 12 about here

CHAPTER IV

GENERAL DISCUSSION

Over the past decade, several laboratory studies have revealed that the human observer is quite good at using visual motion to determine the direction of heading, changes in the direction of heading, and discriminating between self-motion paths. However, most of these studies were conducted with simulated optic flow patterns depicting an environment that was stationary, void of moving objects. While these studies have generated much useful information, it is possible that the results may not generalize to performance in more complex, everyday situations within a dynamic environment.

The few studies that have looked at the effects of moving objects on self-motion judgments have revealed only small effects, even for large moving objects. But these studies did not explore several seemingly important variables, such as the velocity of the object and observer. In our first set of experiments we explored how the velocity of a moving object affects an observer's ability to use the optic flow pattern to discriminate curvilinear from rectilinear self motion. We determined the minimum deviation from a straight path (i.e., the threshold angular speed). Our results showed that when an object moving in depth moves considerably faster (20 m/sec) than the observer its presence detrimentally affects the ability to discrimination self-motion paths. Objects moving in depth at a speed slower or equal to the speed of the observer do not hinder performance.

These findings have important implications for the Air Force mission. A specific objective of this proposal was to determine factors that affect the ability to perceive self-motion paths. This study has identified a condition where path-discrimination performance is significantly degraded, namely when an object moves in depth and at a faster speed than the observer.

In operations of aircraft control or target acquisition, the misperception of direction and/or speed of motion could produce serious errors in the pilot's performance. The results from our second set of experiments indicate that judgments of object velocity made while making eye movements are different from the judgments made with stationary eyes. Significant implications for the Air Force mission follow from these data. If it is universally true that eye movements affect

observers' perception of object velocity, then under conditions when it is critical that a pilot judge the speed of an object moving independently of the aircraft eye movements need to be minimized.

In addition to identifying several stimulus characteristics that affect judgments of velocity while making eye movements, we examined the mechanism underlying the combination of eye movement signals and visual motion signals. Specifically we tested the hypothesis that an extra-retinal signal combines with retinal velocity in a linear manner to determine perceived velocity. We introduced a method to control the retinal velocity in the presence of eye movements for the purpose of determining separate contributions of the retinal-velocity signal and the extra-retinal signal for the perception of stimulus velocity. We also introduced and demonstrated the feasibility of a working model that we developed for how the visual system compensates the changes in the retinal-image motion caused by smooth pursuit eye movements. The findings demonstrated that the traditional views of a linear combination of an extra-retinal and retinal velocity signal for the perception of velocity is unable to explain velocity judgments made while making eye movements. A more complex model is needed, like the one we proposed, in which the compensating eye velocity signal is modified by the retinal velocity prior to combination.

REFERENCES

Crane, H. D., & Steele, C. M. (1985). Generation-V dual-Purkinje-image eyetracker. *Applied Optics, 24*, 527-537.

Cutting, J. E., Vishton, P. M., & Braren, P. A. (1995). How we avoid collisions with stationary and moving obstacles. *Psychological Review, 102*, 627-651.

de Graaf, B., & Wertheim, A. H. (1988). The perception of object motion during smooth pursuit eye movements: adjacency is not a factor contributing to the Filehne illusion. *Vision Research, 28*, 497-502.

Ehrenstein, W. H., Mateef, S., & Hohnsbein, J. (1987). Influence of exposure duration on the strength of the Filehne illusion. *Perception, 16*, 253.

Freeman, T. C. A., & Banks, M. S. (1998). Perceived head-centric speed is affected by both extra-retinal and retinal errors. *Vision Research, 38*, 941-946.

Gibson, J. J. (1950). *Perception of the Visual World.* Boston, Mass.: Houghton Mifflin.

Haarmeier, T., & Thier, P. (1996). Modification of the Filehne illusion by conditioning visual stimuli. *Vision Research, 36*, 741-750.

Mack, A., & Herman, E. (1972). A new illusion: the underestimation of distance during pursuit eye movements. *Perception & Psychophysics, 12*, 471-473.

Riemersma, J. B. J. (1981). Visual control during straight road driving. *Acta Psychologica, 48*, 215-225.

Royden, C. S., & Hildreth, E. C. (1996). Human heading judgments in the presence of moving objects. *Perception and Psychophysics, 58*, 836-856.

Turano, K. A., & Heidenreich, S. M. (1998). Stimulus size influences the effect of eye movements on perceived speed. *Optical Society Technical Program*, 111.

Turano, K. A., & Wang, X. (1994). Visual discrimination between a curved and straight path of self motion: effects of forward speed. *Vision Research, 34*, 107-114.

Turano, K. T., & Heidenreich, S. M. (1999). Eye movements affect the perceived speed of visual motion. *Vision Research, 39*, 1177-1188.

von Helmholtz, H. (1962). *Treatise on physiological optics.* (Vol. III (trans. from the 3rd German ed., JPC Southall)). New York: Dover.

von Holst, E. (1954). Relations between the central nervous system and the peripheral organs. *British Journal of Animal Behaviour, 2*, 89-94.

Warren, W. H., & Hannon, D. J. (1988). Direction of self-motion is perceived from optical flow. *Nature, 336*, 162-163.

Warren, W. H., Morris, M. W., & Kalish, M. (1988). Perception of translational heading from optical flow. *Journal of Experimental Psychology: Human Perception and Performance, 14*, 646-660.

Warren, W. H., & Saunders, J. A. (1995a). Perceived heading depends on the direction of local object motion. *Investigative Ophthalmology and Visual Science, Supplement, 36*, S829.

Warren, W. H., & Saunders, J. A. (1995b). Perceiving heading in the presence of moving objects. *Perception, 24*, 315-331.

Wertheim, A. H., & Van Gelder, P. (1990). An acceleration illusion caused by underestimation of stimulus velocity during pursuit eye movements: Aubert-Fleischl revisited. *Perception, 19*, 471-482.

Appendix 1

Personnel supported and/or associated with effort.

Kathleen A. Turano	Principal Investigator
Peter Kramer	Post-doctoral Research Fellow
Susan M. Heidenreich	Collaborator Associate Professor University of San Francisco, CA
Robert W. Massof	Collaborator Wilmer Eye Institute

Appendix 2

Publications stemming from the research effort.

Journal Articles

Kim, J. and Turano, K.A. (1999) Optimal spatial frequencies for discrimination of motion direction in optic flow patterns. Vision Research, 39, 3175-3186.

Turano, K. A., and Heidenreich, S.M. (1999) Eye movements affect the perceived speed of visual motion. Vision Research, 39, 1177-1187.

Turano, K.A. and Massof, R.W. Nonlinear contribution of eye velocity to motion perception. Submitted to Vision Research.

Published Abstracts

Turano, K.A. and Massof, R.W. (1999) Nonlinear contribution of eye velocity to motion perception. Investigative Ophthalmology & Visual Science (Suppl.), *40*.

Turano, K. A. and Heidenreich, S.M. (1998) Stimulus size influences the effect of eye movements on perceived speed. Optical Society of America Technical Program, 111.

Kramer, P. and Turano, K. A. (1998) Discrimination of curvilinear self-motion from rectilinear self-motion with simulated eye rotation. Investigative Ophthalmology & Visual Science (Suppl), 39, S1083.

Kramer, P. and Turano, K. A. (1998) Effect of object velocity on the discrimination of curvilinear from rectilinear self motion. Perception (Suppl.), 27.

Figure 1

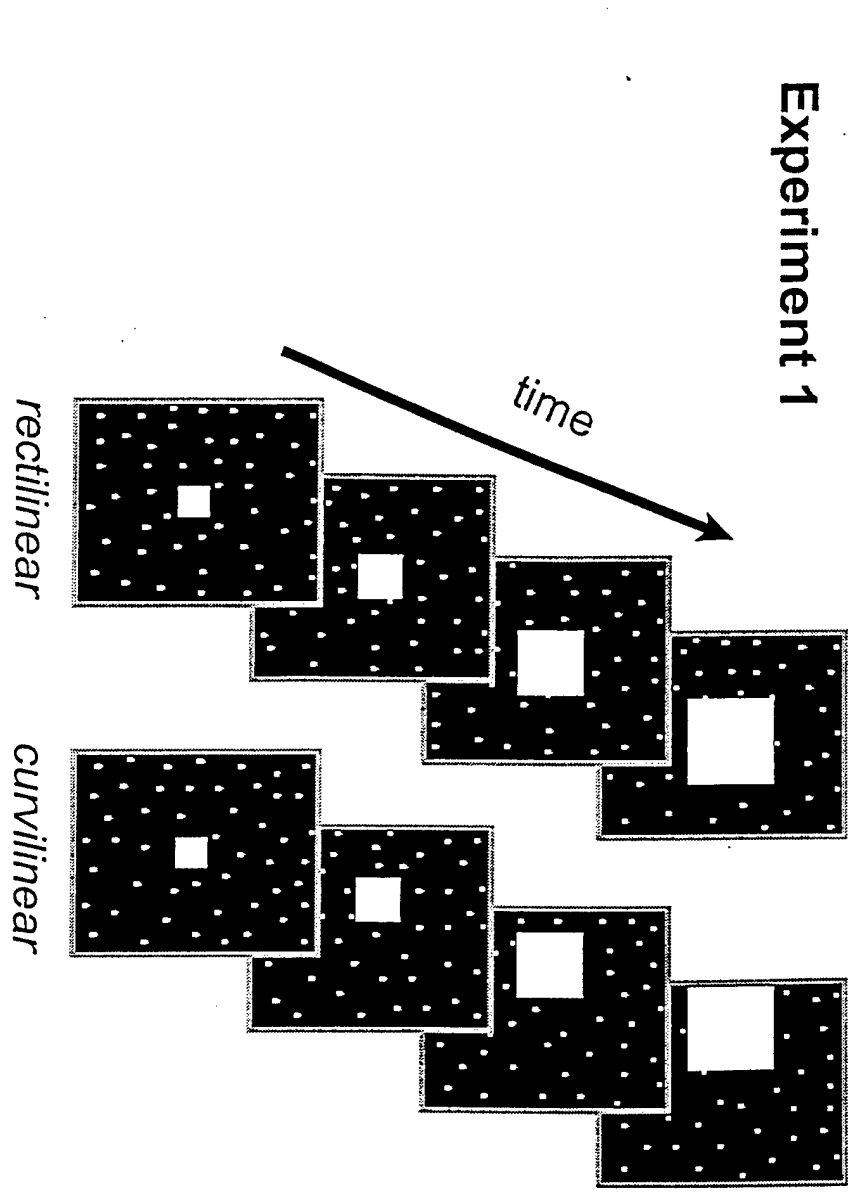

Figure 2

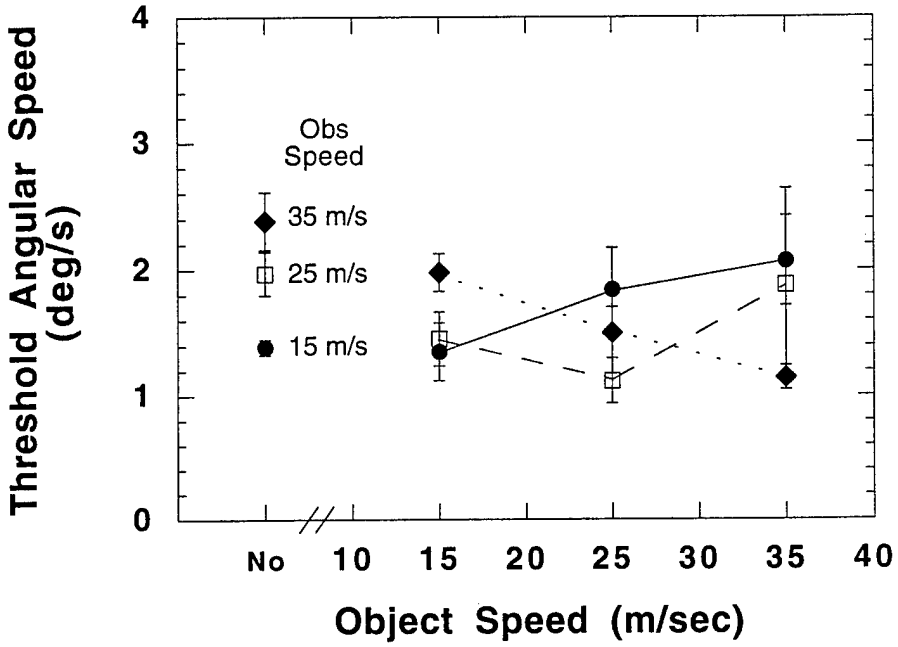
Threshold Angular Speed (deg/s)
4
3
2
1
0
Obs Speed
35 m/s
25 m/s
15 m/s
No
10
15
20
25
30
35
40
Object Speed (m/sec)

Figure 3

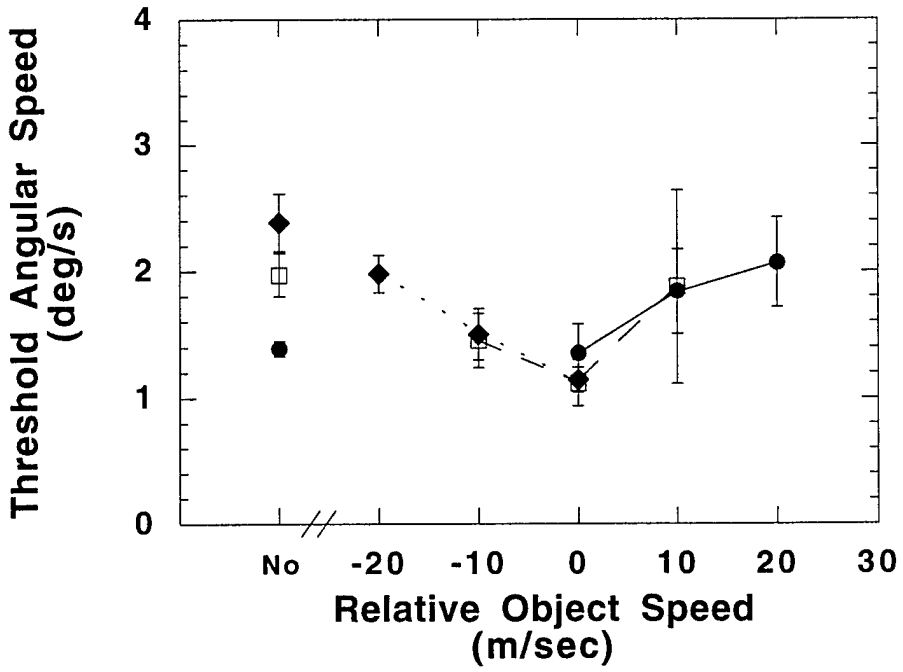
Threshold Angular Speed
(deg/s)
4
3
2
1
0
No
-20
-10
0
10
20
30
Relative Object Speed
(m/sec)

Figure 4

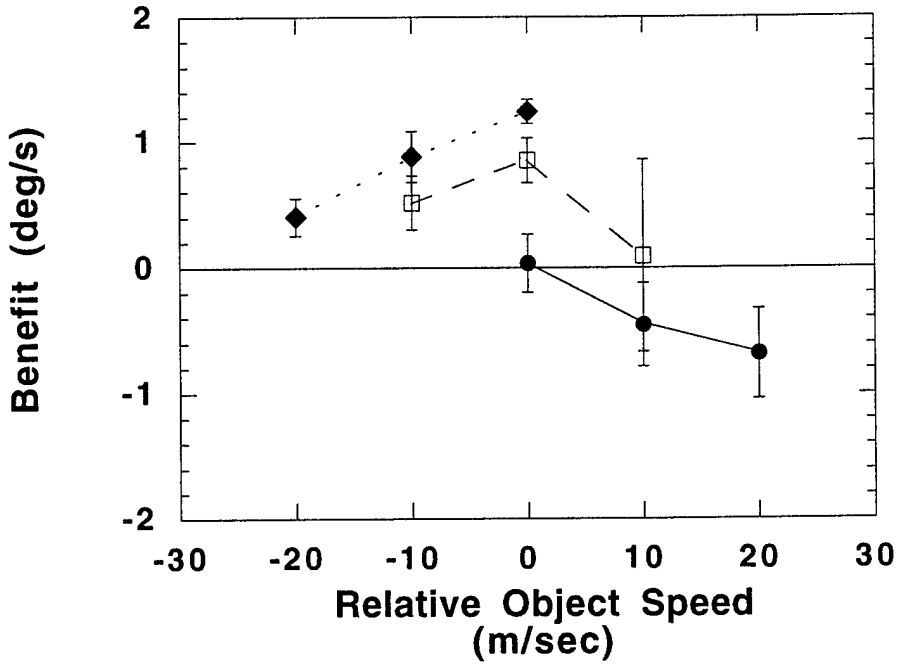
Benefit (deg/s)
2
1
0
-1
-2
-30
-20
-10
0
10
20
30
Relative Object Speed
(m/sec)

Figure 5

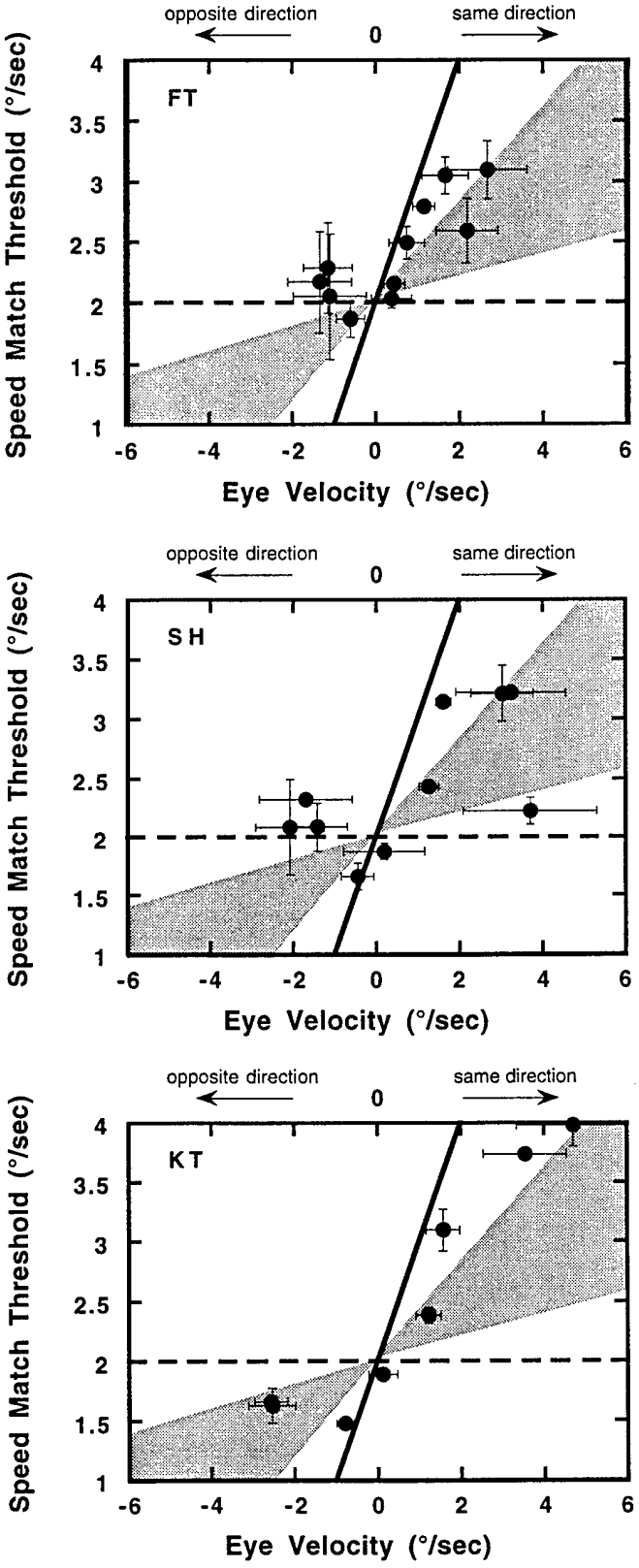
opposite direction
same direction
0
FT
SH
KT
Speed Match Threshold (°/sec)
Eye Velocity (°/sec)
4
3.5
3
2.5
2
1.5
1
-6
-4
-2
0
2
4
6

Figure 6

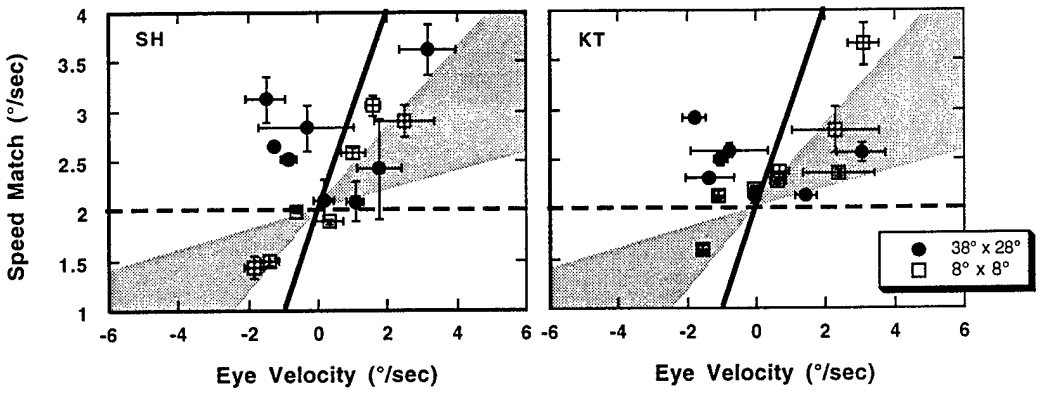
SH
KT
Speed Match (°/sec)
Eye Velocity (°/sec)
Eye Velocity (°/sec)
38° x 28°
8° x 8°
4
3.5
3
2.5
2
1.5
1
-6
-4
-2
0
2
4
6

Figure 7

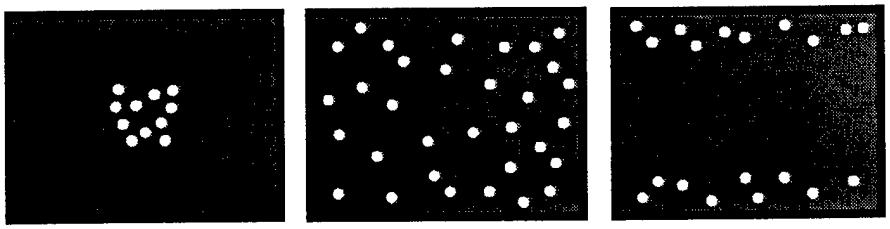

A B C

Figure 8

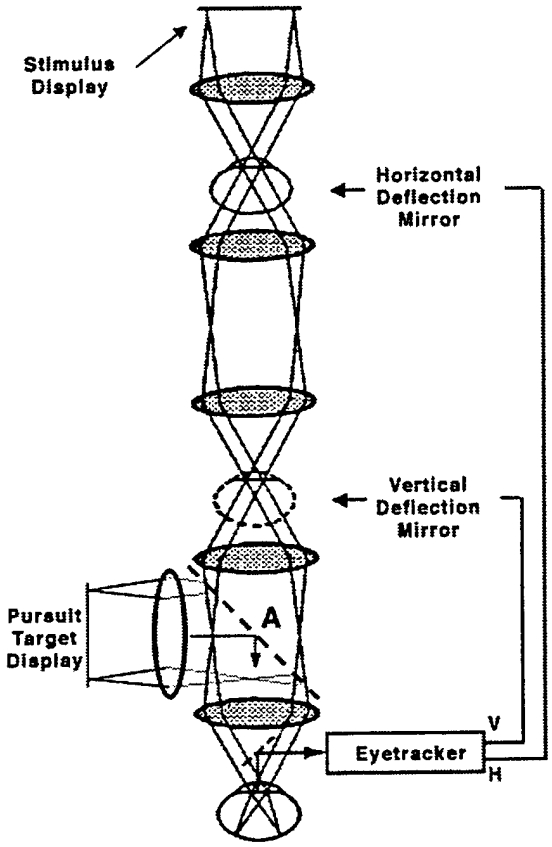
Stimulus Display
Horizontal Deflection Mirror
Vertical Deflection Mirror
Pursuit Target Display
A
V
Eyetracker
H

Figure 9

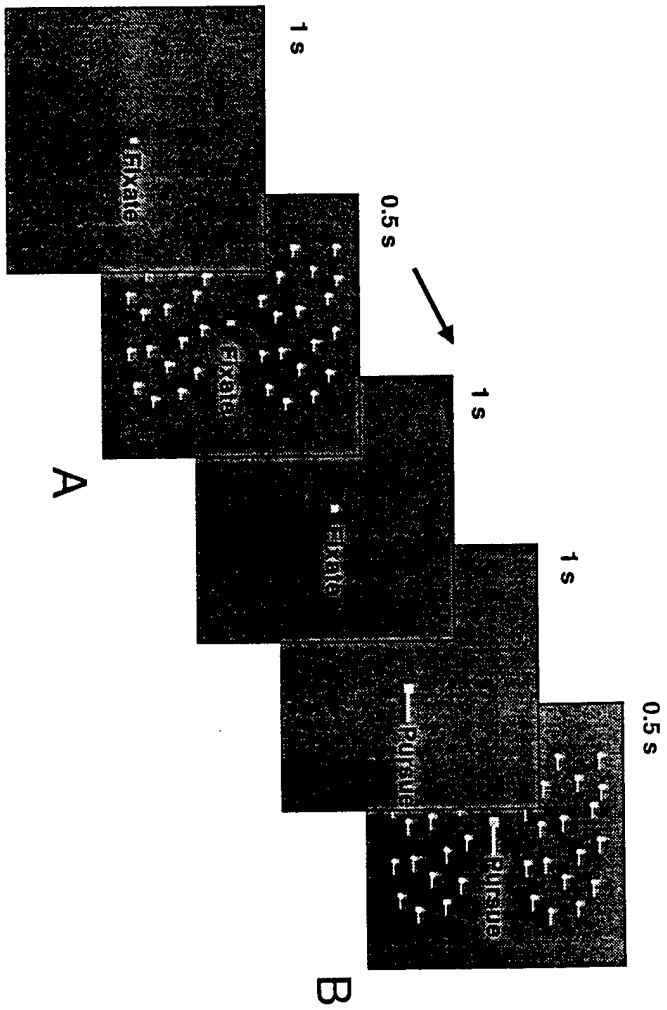
1 s
Fixation
0.5 s
Fixation
1 s
Fixation
A
1 s
Purple
0.5 s
Purple
B

Figure 10

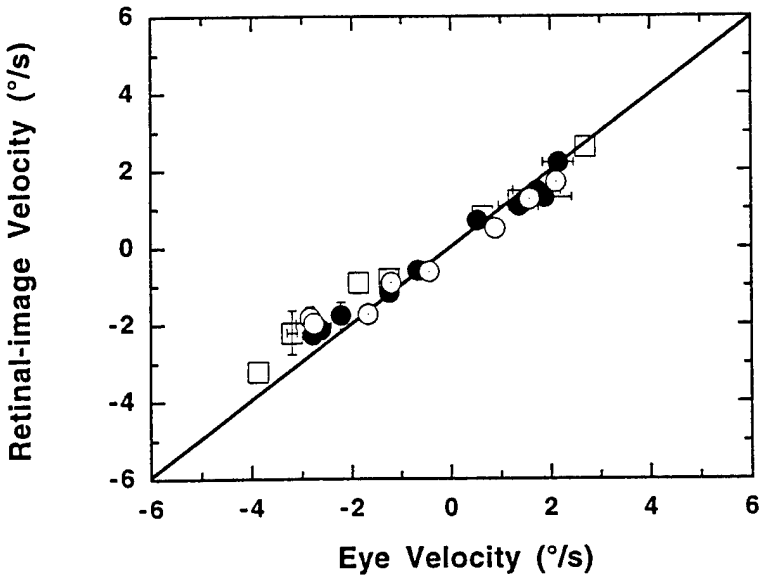

Figure 11

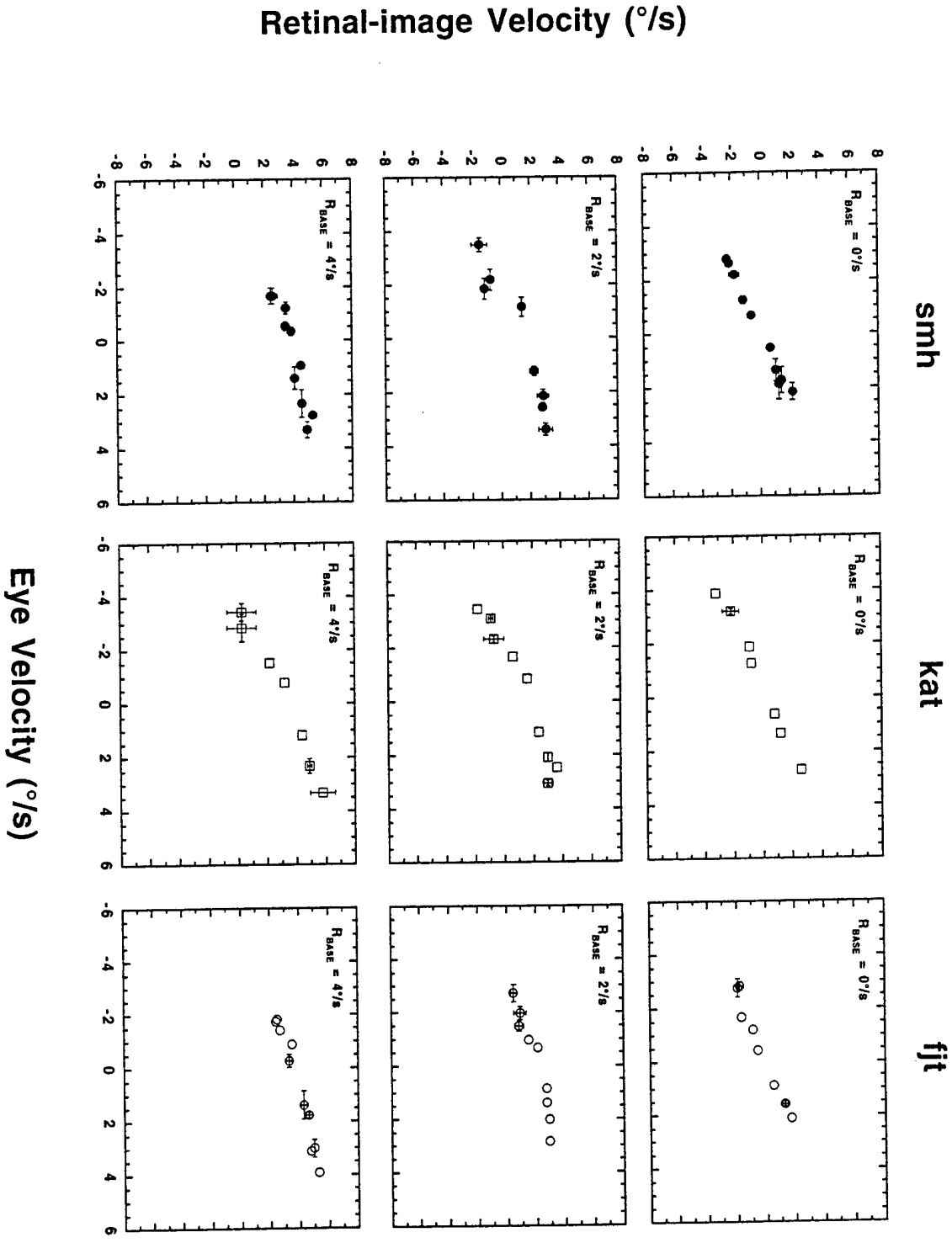
Retinal-image Velocity (°/s)
smh
kat
fjt
Eye Velocity (°/s)
R_BASE = 0°/s
R_BASE = 2°/s
R_BASE = 4°/s

Figure 12

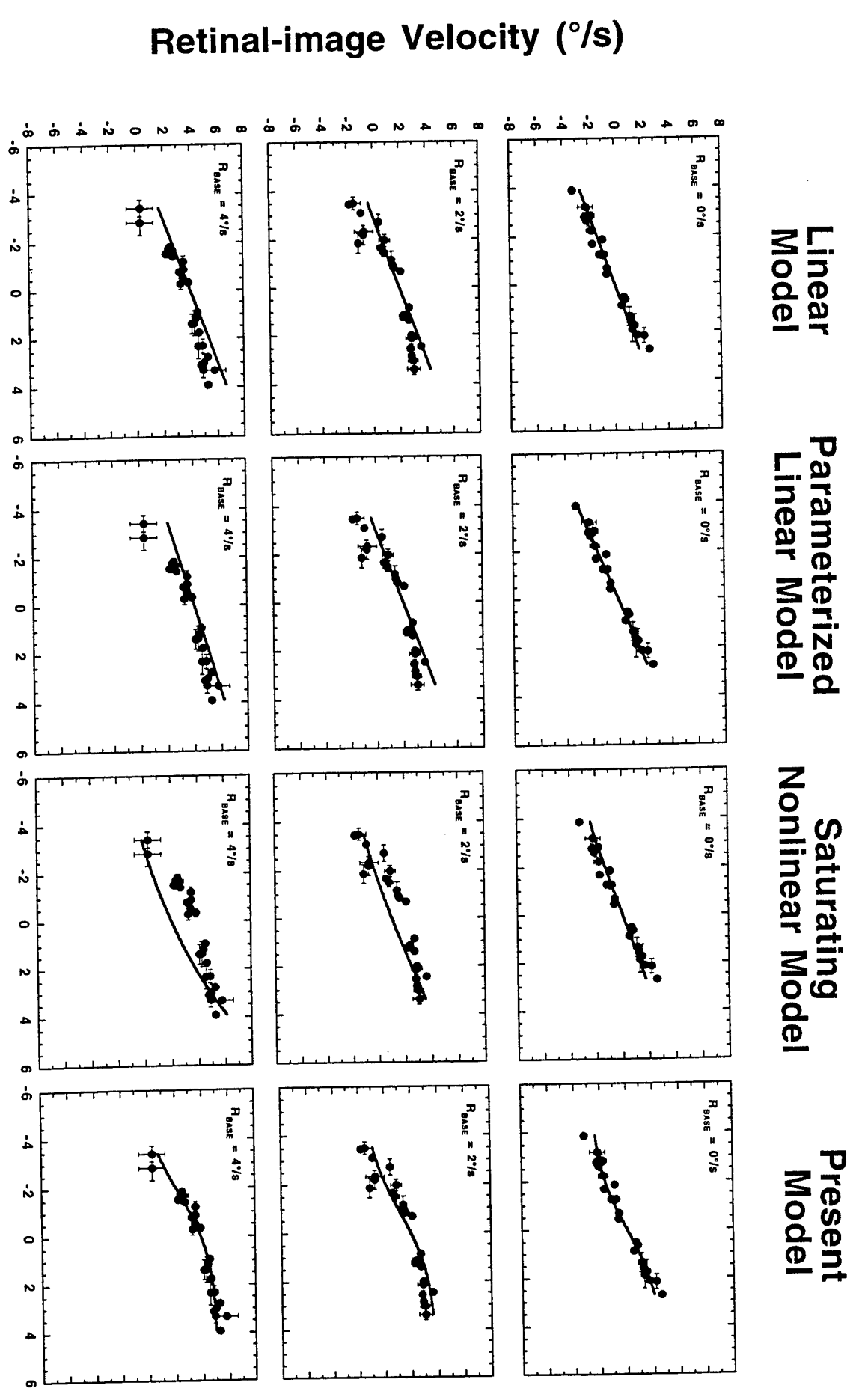
Retinal-image Velocity (°/s)
Linear Model
Parameterized Linear Model
Saturating Nonlinear Model
Present Model
R_BASE = 0°/s
R_BASE = 2°/s
R_BASE = 4°/s
Eye Velocity (°/s)

PERGAMON

Vision Research 39 (1999) 3175–3185

Vision Research

www.elsevier.com/locate/visres

Section 2

Optimal spatial frequencies for discrimination of motion direction in optic flow patterns

Jeounghoon Kim, Kathleen A. Turano *

Wilmer Eye Institute, The Johns Hopkins University School of Medicine, Baltimore, MD 21205, USA

Received 20 July 1998; received in revised form 8 December 1998

Abstract

Spatial frequency tuning functions were measured for direction discrimination of optic flow patterns. Three subjects discriminated the direction of a curved motion path using computer generated optic flow patterns composed of randomly positioned dots. Performance was measured with unfiltered patterns and with patterns that were spatially filtered across a range of spatial frequencies (center spatial frequencies of 0.4, 0.8, 1.6, 3.2, 6.4, and 9.6 c/deg). The same subjects discriminated the direction of uniform, translational motion on the fronto-parallel plane. The uniform motion patterns were also composed of randomly positioned dots, that were either unfiltered or filtered with the same spatial filters used for the optic flow patterns. The peak spatial frequency was the same for both the optic flow and uniform motion patterns. For both types of motion, a narrow band (1.5 octaves) of optimal spatial frequencies was sufficient to support the same level of performance as found with unfiltered, broadband patterns. Additional experiments demonstrated that the peak spatial frequency for the optic flow patterns varies with mean image speed in the same manner as has been reported for moving sinusoidal gratings. These findings confirm the hypothesis that the outputs of the local motion mechanisms thought to underlie the perception of uniform motion provide the inputs to, and constrain the operation of, the mechanism that processes self motion from optic flow patterns.

Keywords: Motion; Curved motion; Optic flow; Direction discrimination; Spatial frequency

1. Introduction

The visual motion patterns that are generated by an observer moving in a rigid environment [referred to as optic flow after Gibson (1950)] are complex velocity patterns. For example, when an observer is moving on a straight path, the velocity vectors radiate outward from a common point of origin that is coincident with the observer's instantaneous direction of motion. The speed of the vectors increases from the point of origin outward and is dependent on the speed of the observer, as well as on the position of the underlying environmental element. Studies have shown that human observers can use these optic flow patterns to determine the direction of heading (Cutting, 1986; Warren & Hannon, 1988; Warren, Morris & Kalish, 1988; Warren & Hannon, 1990; Royden, Banks & Crowell, 1992; van den Berg, 1992; Crowell & Banks, 1993; Perrone & Stone, 1994; Royden, Crowell & Banks, 1994). When an observer moves on a curvilinear path, the motion pattern becomes even more complex due to the added rotation component. Studies have shown that human observers are able to detect small changes in the direction of heading (Riemersma, 1981; Turano & Wang, 1994; Turano, 1995) as well as the direction of the curvilinear motion paths (Warren, Mestre, Blackwell & Morris, 1991).

It is hypothesized that the mechanisms that compute motion from the optic flow patterns are fed by local motion mechanisms that encode uniform, translational motion on the fronto-parallel plane (Orban, Laae, Verri, Raiguel, Xiao, Maes et al., 1992; Perrone, 1992;

* Corresponding author. Tel.: +1-410-5026434; fax: +1-410-9551829.

E-mail address: kathy@lions.med.jhu.edu (K.A. Turano)

0042-6989/99/$ - see front matter
PII: S0042-6989(99)00024-3

Verri, Straforini & Torre, 1992; Lappe & Rauschecker, 1993; Perrone & Stone, 1994; Warren & Saunders, 1995). If this is true, we expect the processing of optic flow and uniform motion to be constrained by the same operating limits.

The spatial frequency tuning curve for uniform motion has been determined for sinusoidal gratings (Kelly, 1979; Wilson, 1985; Burr & Ross, 1982), gabor patches (Watson & Turano, 1995), and biphasic sinusoidal bars (Burr & Ross, 1982). With these motion patterns, contrast sensitivity has been shown to vary in an inverted U shaped manner with spatial frequency, and the peak of the spatial frequency tuning curve depends on the pattern's speed. The faster the speed the lower the peak spatial frequency.

Given the heterogeneity of speeds in the optic flow patterns, a question arises concerning the shape and peak location of the spatial frequency tuning curve for the mechanism that processes self motion from the optic flow patterns. It may be that the spatial frequency tuning curve for optic flow patterns is a broad envelope encompassing the peaks of the tuning curves that correspond to each speed represented in the optic flow pattern. Another possibility is that the tuning curves for the optic flow and uniform motion patterns are similar in shape and peak frequency when the mean image speed of the optic flow speed distribution matches the speed of the uniform motion pattern. Support for this comes from a study that showed that human observers base speed judgments on the mean speed when presented with a stimulus of heterogenous speeds (Watamaniuk & Duchon, 1992). Furthermore, changes in the mean speed of complex motion patterns have been shown to modulate the neuronal responses in the area of monkey cortex believed to be responsible for optic flow processing (Duffy & Wurtz, 1997).

The spatial frequency characteristics of the mechanisms that underlie the perception of self motion from optic flow patterns are relatively unknown. In a preliminary investigation, Sekuler (1991) found that speed discrimination thresholds obtained with optic flow patterns that were blurred with a five diopter lens were similar to the thresholds obtained with unblurred patterns. Sekuler (1991) suggested that low spatial frequency information may be sufficient for processing self motion information from optic flow. Unfortunately, Sekuler did not test patterns in which only the spatial frequency content and not the contrast was manipulated, nor did she test patterns restricted to medium or high spatial frequencies.

If the spatial frequency tuning curve for optic flow patterns corresponds to the tuning curve for uniform motion patterns, there would be confirmation of the general expectation that the outputs of the local motion mechanisms, thought to underlie the perception of uniform motion, provide the inputs to the optic flow computations. We would then be able to generalize findings of earlier studies performed with simpler stimuli to the more complex case of optic flow.

In Experiment 1, we measured subjects' ability to discriminate the direction of circular paths of motion using optic flow patterns that were spatial frequency filtered across a range of center spatial frequencies. The spatial frequency tuning curve obtained with the filtered optic flow patterns was compared to the tuning curve for uniform motion patterns at the mean image speed of the optic flow patterns.

2. Experiment 1: effect of center spatial frequency on direction discrimination using optic flow and uniform motion patterns

2.1. Methods

2.1.1. Stimuli

The *optic flow* patterns were computer generated motion sequences simulating an observer moving relative to a volume ($35 \times 35 \times 100$ m) of dots whose positions were randomly sampled from a uniform distribution. Observer motion was simulated by projecting the dots onto a plane that remained positioned at a distance of 40 cm along the observer's line of sight. The initial position of the projection plane was at the front surface of the volume. As the dots passed by the observer they disappeared and did not reappear at the back of the volume. The edges of the volume were never visible. Each dot was composed of 2×2 pixels and subtended a visual angle of 4.6×4.6 arcmin. The mean speed of the dots in the optic flow patterns projected on the image plane was 2.3 deg/s. The size of the square image (256×256 pixels) subtended a visual angle of $10° \times 10°$ at the viewing distance of 40 cm. The optic flow patterns occupied approximately 1/16th of the total screen (1280×1024 pixels). The average number of dots per frame was 160, producing an average dot density of 1.6 dots/deg^2. The dots were white (72.4 cd/m^2) and the background was black (4.7 cd/m^2). Accurate levels of contrast were achieved by using a video attenuator that combined the outputs of the board's eight bit digital to analog converters (Pelli & Zhang, 1991). The video attenuator and monitor were calibrated to linearize a range of voltage luminance values.

A circular path of motion was created by moving the positions of the projection plane and the observer's viewpoint forward along the observer's line of sight and then rotating them with respect to a vertical axis passing through the observer's viewpoint (cf. Turano & Wang, 1994). The size of the forward step was determined by the simulated forward speed of 15 m/s. The direction of the forward motion relative to the center of

the display was randomized (± 1.0, ± 0.5, or 0°). The radius of the circular path was 2578 m. The rotation angle was 0.18°, approximately 1.6 times the angular discrimination threshold as established during pilot testing. A 533 ms motion sequence consisted of 16 frames presented at a rate of 30 frames/s.

The *uniform motion* patterns consisted of dots whose positions were randomly sampled from a uniform distribution of dots on a fronto-parallel plane. The positions of the dots translated in a standard direction (either 20 or 160°—rightward horizontal motion defined as 0°) or in a test direction ($\pm 5°$ from the standard direction. The direction difference of 5° is approximately 1.6 times direction discrimination threshold as established during pilot testing). The dots translated together behind a 10° circular aperture at a viewing distance of 40 cm. The dots were the same size and luminance as in the optic flow patterns. The average number of dots per frame was 125. Dot speed was 2.2 deg/s.

The optic flow and uniform motion patterns were filtered with the fast Fourier transform routine provided in MatLab (MathWorks, Inc., Natick, MA). The filters were 2D Gaussians with a bandwidth (1D) of 1.5 octaves at half height, full width. Grey levels were normalized to maintain a constant global contrast level across filtered stimuli. The luminance of the minimum grey level was 4.7 cd/m^2, and the luminance of the maximum grey level was 72.4 cd/m^2. Thus contrast, when calculated as $(L_{max} - L_{min})/L_{min}$, was 14.4. (In this and all subsequent experiments, the subjects were able to detect the stimulus; stimulus visibility did not limit performance.) Judgments were made for six center spatial frequencies (0.4, 0.8, 1.6, 3.2, 6.4, and 9.6 c/deg). Fig. 1 shows the one dimensional profile of the Gaussian filters together with each of three spatially filtered dot patterns.

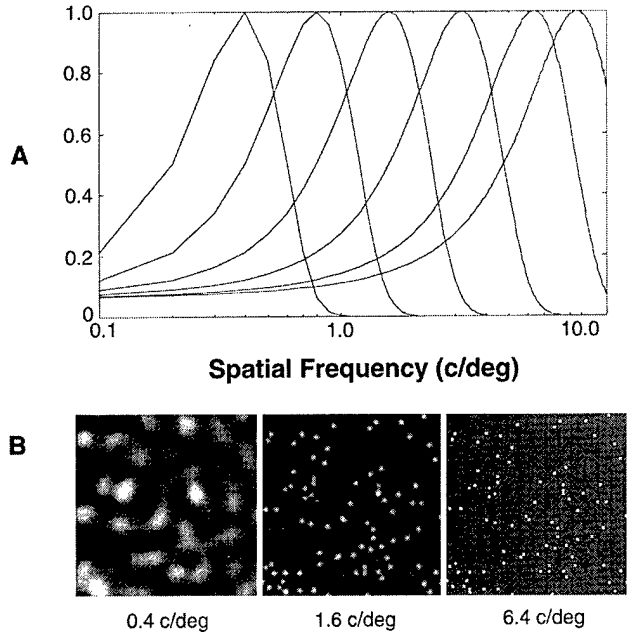

Fig. 1. (A) One-dimensional profile of the Gaussian filters. (B) One frame from filtered optic flow patterns with center spatial frequencies of 0.4, 1.6, and 6.4 c/deg.

2.1.2. Procedure

In the optic flow sessions, a trial began with a tone followed by the presentation of a motion sequence of optic flow. The optic flow simulated self motion on a leftward-counterclockwise (Fig. 2a) or rightward-clockwise (Fig. 2b) circular path. The subject's task was to indicate, by pressing the left or right mouse button, the direction of motion relative to a straight motion path.

In the uniform motion sessions, a trial began with a tone followed by the presentation of two successive movies of uniform motion. In one movie, dots moved in the standard direction, and in the other movie they moved in a test direction. The standard direction and order were randomly determined for each trial. The subject's task was to indicate the movie in which the motion direction was more vertical.

No feedback was given. The subject viewed the display monocularly with his/her chin and forehead positioned on a headrest. The subject was instructed to look toward the center of the screen. Eye movements were not monitored. Overhead lights were turned off, and the only light in the room came from the display and a small desk lamp. We used the method of constant stimuli with the spatially filtered patterns to determine the effect of center spatial frequency on direction discrimination. Each center frequency was presented 20 times in a random order, and each subject participated in two sessions. Mean thresholds are reported.

2.1.3. Apparatus

A Power Macintosh 6100/66 was used to generate the patterns which were then transferred to a Silicon Graphics Iris 4D/IRIX workstation for display. The patterns were displayed on an 19″ Ikegami monochrome monitor with P104 phosphor (Model 1210P; Ikegami Electronics, Inc., Maywood, NJ). The refresh rate was 60 Hz, non interlaced, and pixel resolution was 1280 × 1024.

2.1.4. Subjects

Three individuals with normal or corrected-to-normal vision served as subjects. Two of the subjects were the authors, and the third subject was an inexperienced psychophysical observer.

2.2. Results

Fig. 3 shows the proportion correct responses for direction discrimination for the spatially filtered optic

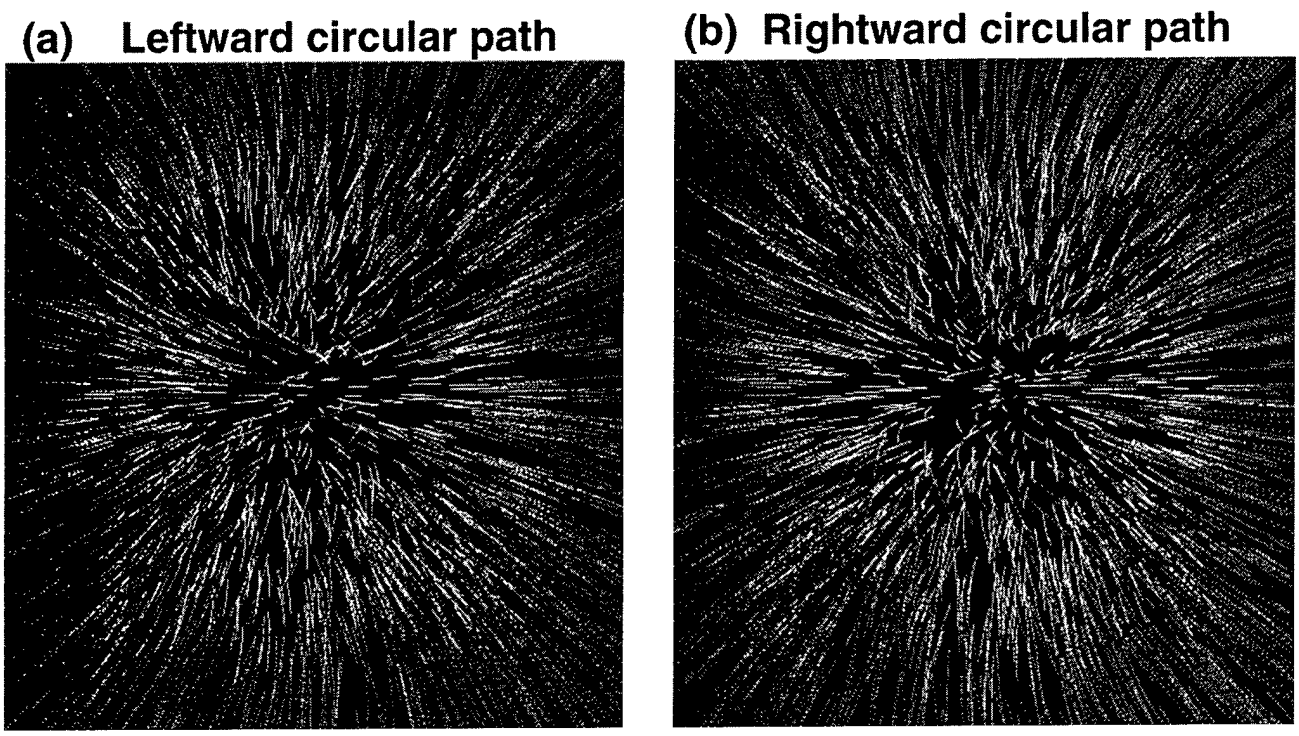

Fig. 2. Time exposure of optic flow patterns that simulate the visual motion generated as a person moves along a (a) leftward-counterclockwise or (b) rightward-clockwise circular motion path.

flow patterns plotted as a function of center spatial frequency. For all subjects, performance varied in an inverted U shaped manner as a function of center spatial frequency. Peak performance was achieved at a spatial frequency of 1.6 c/deg. At spatial frequencies of 0.4 and 9.6 c/deg, performance was decreased by about 25%. These results indicate that some spatial frequencies are more effective than others in relaying information about motion paths. Specifically, with the stimulus dimensions that we used, motion information centered at 1.6 c/deg is the most effective spatial frequency range to achieve accurate direction discrimination using optic flow patterns.

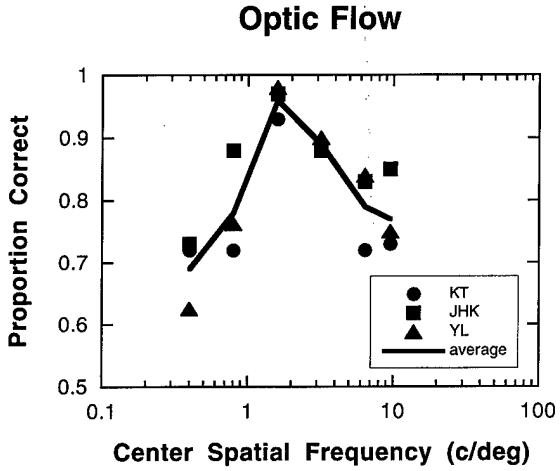

Fig. 3. Proportion of correct responses for direction discrimination of a circular motion path (rotation angle = 0.18°) plotted as a function of center spatial frequency. Each symbol indicates data from one subject. The solid line connects the mean proportion correct response averaged across subjects. Peak spatial frequency was 1.6 c/deg.

The data just discussed demonstrate that a narrow band of spatial frequencies, optimally placed, is sufficient to achieve accurate direction discrimination for suprathreshold levels of circular motion. To determine whether this narrow band of spatial frequencies is sufficient to achieve the same direction discrimination thresholds as with broadband stimuli, we determined the angular threshold for direction discrimination using optic flow patterns whose spatial frequency was restricted to 1.5 octaves centered at 1.6 c/deg and compared it to the angular threshold using unfiltered optic flow patterns.

Fig. 4 shows each subject's proportion of correct responses for direction discrimination plotted against the rotation angle of the circular motion path. The open symbols represent data obtained with the unfiltered patterns, and the closed symbols represent data obtained with the filtered patterns. The lines indicate the best fit Weibull functions (Weibull, 1951). The mean of the three subjects' angular thresholds obtained with the filtered patterns is 0.11°, the same as the average threshold obtained with the unfiltered patterns. These results indicate that motion information carried by this narrow band of spatial frequencies is sufficient

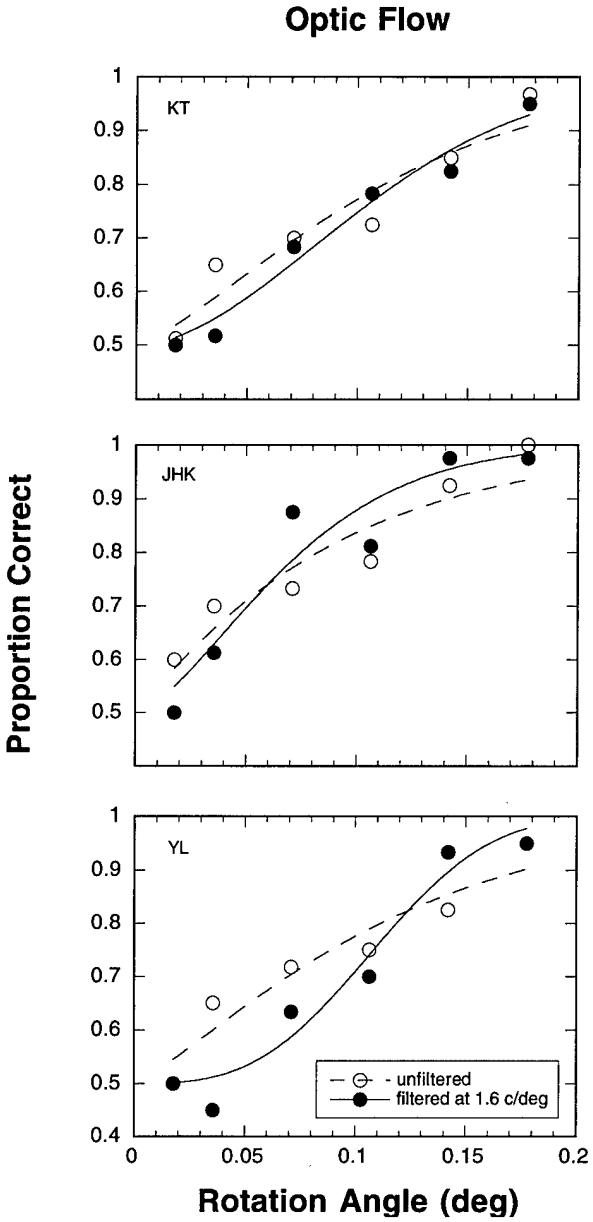

Fig. 4. Proportion of correct responses for direction discrimination plotted against the rotation angle of the optic flow patterns. The open symbols represent data obtained with the unfiltered patterns and the closed symbols represent data obtained with the filtered patterns. The lines indicate the best-fit Weibull functions.

for subjects to achieve the same level of direction discrimination performance as obtained with the broadband stimuli. Performance did not suffer when the spatial frequency content of the optic flow patterns was restricted to a narrow band of frequencies centered at 1.6 c/deg.

For the uniform motion patterns, proportion correct responses is plotted as a function of center spatial frequency in Fig. 5. The pattern of results is similar to that obtained with the optic flow patterns; performance varied in an inverted U shaped manner as a function of center spatial frequency. Peak performance was achieved at the same spatial frequency, 1.6 c/deg, as found with the optic flow patterns.

As we did with the optic flow patterns, we determined the threshold for direction discrimination using uniform motion patterns whose spatial frequency content was restricted to 1.5 octaves centered at 1.6 c/deg and compared it to the threshold using unfiltered uniform motion patterns. Fig. 6 shows each subject's proportion vertical response plotted against the direction difference of the uniform motion patterns. The open symbols represent data obtained with the unfiltered patterns, and the closed symbols represent data obtained with the filtered patterns. The lines indicate the best fit Weibull functions. The average of the three subjects' thresholds for the filtered patterns is 2.7°, similar to the 2.8° threshold obtained with the unfiltered patterns. These results indicate that motion information carried by this narrow band of spatial frequencies is sufficient for subjects to achieve the same level of direction discrimination performance as obtained with the broadband stimuli. Performance did not suffer when the spatial frequency content of the uniform motion patterns was restricted to a narrow band of frequencies centered at 1.6 c/deg. Thus, for direction discrimination of both the uniform motion and optic flow patterns, the peak center frequency is the same (i.e. 1.6 c/deg) and there is no loss in performance with an optimally placed, narrow spatial frequency band.

3. Experiment 2: effect of optic flow speed on spatial frequency tuning

The results of Experiment 1 identified 1.6 c/deg as the peak of the spatial frequency tuning function for optic flow patterns whose mean image speed was 2.3 deg/s

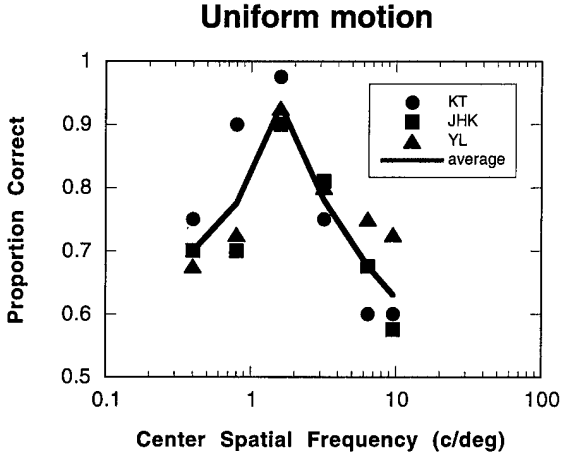

Fig. 5. Proportion of correct responses for direction discrimination of uniform motion (direction difference = 5 deg) plotted as a function of center spatial frequency. The solid line connects the mean proportion correct response averaged across subjects. Peak spatial frequency was 1.6 c/deg.

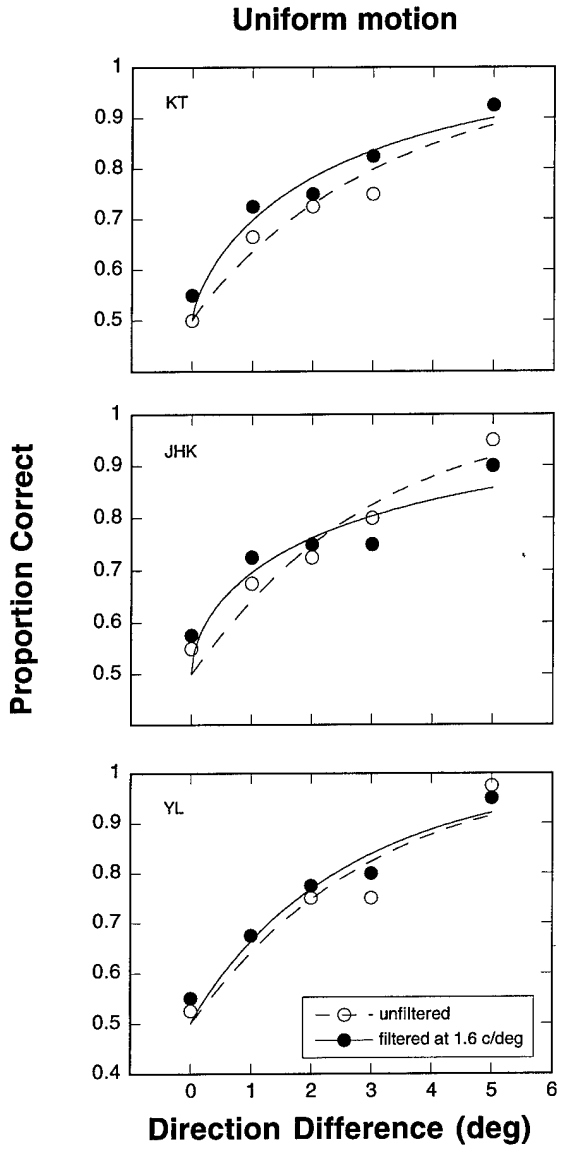

Fig. 6. Proportion of vertical responses for direction discrimination plotted against the direction difference of the uniform motion patterns. The open symbols represent data obtained with the unfiltered patterns and the closed symbols represent data obtained with the filtered patterns. The lines depict the best-fit Weibull functions.

and for translating patterns moving at a speed of 2.2 deg/s. In past studies with sinusoidal gratings, similar peak frequencies were found for stimuli that moved at a comparable speed. For example, Kelly (1979) reported a peak spatial frequency of 1.5 c/deg for sinusoidal gratings moving at 3 deg/s, and Burr and Ross (1982) found a peak close to 2 c/deg for a grating moving at 1 deg/s. The similarity in peak spatial frequency between the optic flow patterns and the sinusoidal gratings suggests that the spatial frequency-speed interaction previously reported for sinusoidal gratings may exist with the optic flow patterns. To determine whether the tuning function shifts along the spatial frequency axis with changes in the mean image speed in the same manner as previously reported with sinusoidal gratings (Kelly, 1979; Burr & Ross, 1982; Wilson, 1985), we varied the mean image speed of the optic flow patterns and measured direction discrimination using filtered optic flow patterns.

3.1. Methods

3.1.1. Stimuli and apparatus

Stimuli were optic flow patterns created in the same manner as described above for Experiment 1. In Experiment 1, the forward speed was 15 m/s resulting in a mean image speed of 2.3 deg/s. In this experiment, forward speeds of 5, 15, and 26 m/s were tested in order to look at the effects of the mean image speed on the spatial frequency tuning curve. At the 5 m/s forward speed, the mean image speed of the optic flow patterns was 0.6 deg/s, and at the 26 m/s forward speed, the mean image speed was 9.0 deg/s. Other stimulus conditions and apparatus were identical to those in Experiment 1.

3.1.2. Procedure

The experimental procedure was the same as used in Experiment 1 with the following exceptions. Because angular threshold varies with forward speed (Turano & Wang, 1994), thresholds were determined for each subject to ensure that the rotation angle chosen for each forward speed was above the threshold determined with unfiltered optic flow patterns. Rotation angles were 0.11, 0.18, and 0.32° for forward speeds of 5, 15, and 26 m/s, respectively, each approximately 1.6 times threshold as established during pilot testing. Center spatial frequencies ranged from 0.4 to 9.6 c/deg for the 5 m/s and 15 m/s conditions and from 0.2 to 3.2 c/deg for the 26 m/s condition.

3.1.3. Subjects

Three individuals with normal or corrected-to-normal vision served as subjects. One of the subjects was the first author, one subject was an inexperienced psychophysical observer, and the third subject was an experienced psychophysical observer, naive with respect to the hypothesis of the experiment.

3.2. Results

Fig. 7 shows the proportion of correct responses plotted as a function of center spatial frequency. For the two fastest speeds, performance varied in an inverted U shaped manner as a function of center spatial frequency. Peak performance was obtained at the cen-

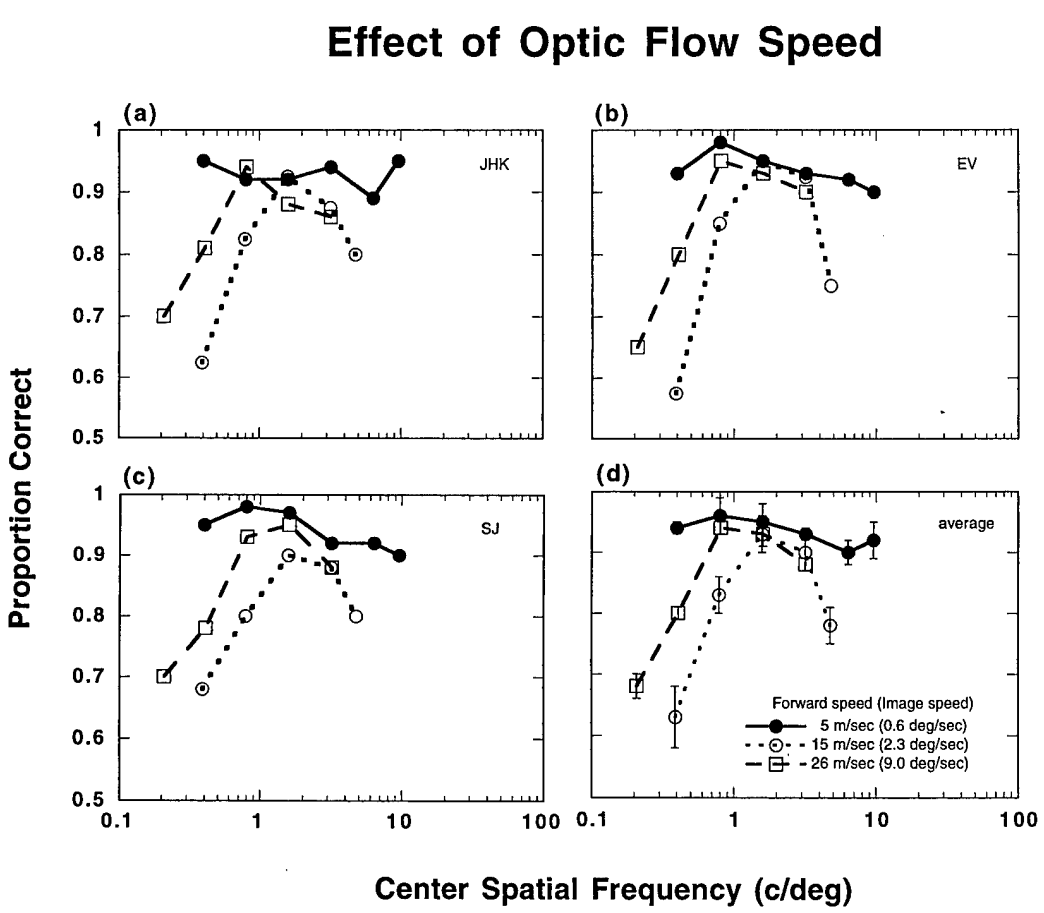

Fig. 7. Proportion of correct responses for direction discrimination of a circular motion path plotted as a function of center spatial frequency. Symbols represent data for optic flow patterns simulating forward speeds of 5 (●), 15 (○), and 26 m/sec (□). Data shown are from subjects (a) JHK; (b) EV; (c) SJ: and (d) the mean across the three subjects. Error bars are ±1 S.E.M.

ter spatial frequency of 1.6 c/deg for the 15 m/s forward speed (mean image speed of 2.3 deg/s) and at 0.8 c/deg for the 26 m/s forward speed (mean image speed of 9.0 deg/s). As the speed of the optic flow patterns increased, the peak of the spatial frequency tuning function decreased. Shifting the 15 m/s curve leftward on the spatial frequency axis by a factor of two results in a relatively good superposition of the two curves at the low spatial frequency end. This spatial frequency shift in the tuning function toward lower spatial frequencies with increasing speed is similar to previous findings with sinusoidal gratings (Kelly, 1979; Burr & Ross, 1982; Wilson, 1985). In Kelly's study, the peak of the contrast sensitivity function for the detection of a grating moving at 3 deg/s was 1.5 c/deg. The peak shifted to 0.5 c/deg for a grating moving at 11 deg/s. In the study by Burr and Ross, the peaks of the contrast sensitivity function were 2–3 c/deg for a grating moving at 1 deg/s and 0.6 c/deg for a grating moving at 10 deg/s. The magnitude of shift that we observed with the optic flow patterns is comparable to those previously reported for sinusoidal gratings.

Performance at the slowest speed was qualitatively different from the performance obtained at the faster speeds. Performance was higher with the slowest optic flow pattern at the non-optimal spatial frequencies compared to performance with the faster optic flow patterns. The function was relatively flat across spatial frequencies; discriminability remained higher than 0.9 across all spatial frequencies. It may be that the position information from the slowest optic flow patterns enabled the subjects to determine the motion direction. Nakayama and Tyler (1981) have shown that for moving elements with recognizable position cues and small change in position, position sensitivity dominates to determine detection threshold.

4. Experiment 3: effect of field of view of optic flow patterns on spatial frequency tuning

Experiment 2 demonstrated that the optimal spatial frequencies of the optic flow patterns for direction discrimination vary depending on the speed of the optic flow. As the speed of the optic flow patterns increased,

the peak of the spatial frequency tuning function decreased. In Experiment 2, the simulated forward speed of the observer and the mean image speed covaried. Given that the shift in spatial frequency tuning was comparable to what has been reported with sinusoidal gratings moving at the mean image speed of the optic flow patterns, it is likely that the critical factor governing the tuning function is not the simulated forward speed, rather it is the mean image speed. One way to dissociate forward speed from mean image speed is to hold constant the forward speed and vary the speeds of randomly selected velocity vectors. The problem with this method is that the optic flow pattern that is produced is not a valid optic flow pattern, and the inconsistencies might influence discrimination performance. An alternative method is to hold constant the forward speed of the optic flow patterns and vary the field of view. Because image speed is fastest in the more peripheral portions of our optic flow patterns, increasing the field of view increases the mean image speed of the optic flow pattern. If mean image speed is critical in determining the optimal spatial frequencies of the optic flow patterns, then the tuning function should shift toward lower spatial frequencies with increasing field of view. We tested this in Experiment 3.

4.1. Methods

4.1.1. Stimuli and apparatus

Stimulus conditions and apparatus were identical to those in Experiment 1, with the following exceptions. Viewing distance, and hence position of projection plane along the observer's line of sight, was held constant at 20 cm. The size of the pattern was 512×512 pixels. The retinal image size was manipulated by either displaying the entire pattern ($40° \times 40°$) or covering the peripheral portion of the display with black matte tape to produce a $10° \times 10°$ display. The mean image speed for the $40° \times 40°$ display was 12.0 deg/s and the mean image speed for the $10° \times 10°$ display was 2.4 deg/s. Rotation angle was 0.27°.

4.1.2. Procedure

The procedure is the same as described in the optic flow section of Experiment 1.

4.1.3. Subjects

The second author and two experienced psychophysical observers, naive with respect to the hypothesis of the experiment, served as subjects. The subjects wore appropriate corrective lenses to equate accommodative demand in this experiment to that in the earlier experiments ($+1.0$D for KT and $+2.5$ D for EV and AD).

4.2. Results

Based on the fact that the mean image speed of the larger field of view ($40° \times 40°$) is faster than the smaller field of view ($10° \times 10°$), we predicted that the peak of the spatial frequency tuning curve would be at a lower spatial frequency for the larger field of view. As shown in Fig. 8, the results support our prediction. Proportion of correct responses for direction discrimination is plotted against the center spatial frequency of the optic flow patterns. The average performance of the three subjects is shown in Fig. 8d. Peak performance was achieved at the center spatial frequency of 1.6 c/deg for the $10° \times 10°$ display and at 0.8 c/deg for the $40° \times 40°$ display. This shift in the peak frequency toward lower spatial frequencies with the larger display size is consistent with the view that the mean image speed affects the spatial frequency tuning of the underlying motion mechanism.

5. Discussion

Spatial frequency tuning functions were measured for direction discrimination using optic flow patterns. The results showed that, with the exception of very slow optic flow patterns where performance was independent of spatial frequency, the ability to discriminate the direction of curvilinear motion paths varied in an inverted U shaped manner as a function of center spatial frequency. With optic flow patterns simulating a 15 m/s forward speed, peak performance occurred with a center spatial frequency of 1.6 c/deg. The same optimal spatial frequency was obtained for direction discrimination using patterns of uniform motion matched to the mean image speed of the optic flow patterns. Moreover, for both types of motion, a narrow band (1.5 octaves) of spatial frequencies centered at 1.6 c/deg was sufficient to achieve the same level of performance as found with the unfiltered, broadband patterns. Our findings that the peaks of the spatial frequency tuning functions and their general shapes were the same for direction discrimination of both optic flow and uniform motion support the general expectation that the outputs of the local motion mechanisms, thought to underlie the perception of uniform motion, provide the inputs to the optic flow computations. Furthermore, the results of Experiments 2 and 3 demonstrate that the same spatial frequency-speed interaction reported for uniform motion of sinusoidal stimuli (Kelly, 1979; Burr & Ross, 1982; Wilson, 1985) occurs with optic flow patterns. The optic flow patterns that simulated the curvilinear motion paths were composed of a translation and rotation component. One would expect that the same tuning functions will describe heading discrimination with optic flow patterns that contain only a translation component. This remains to be determined.

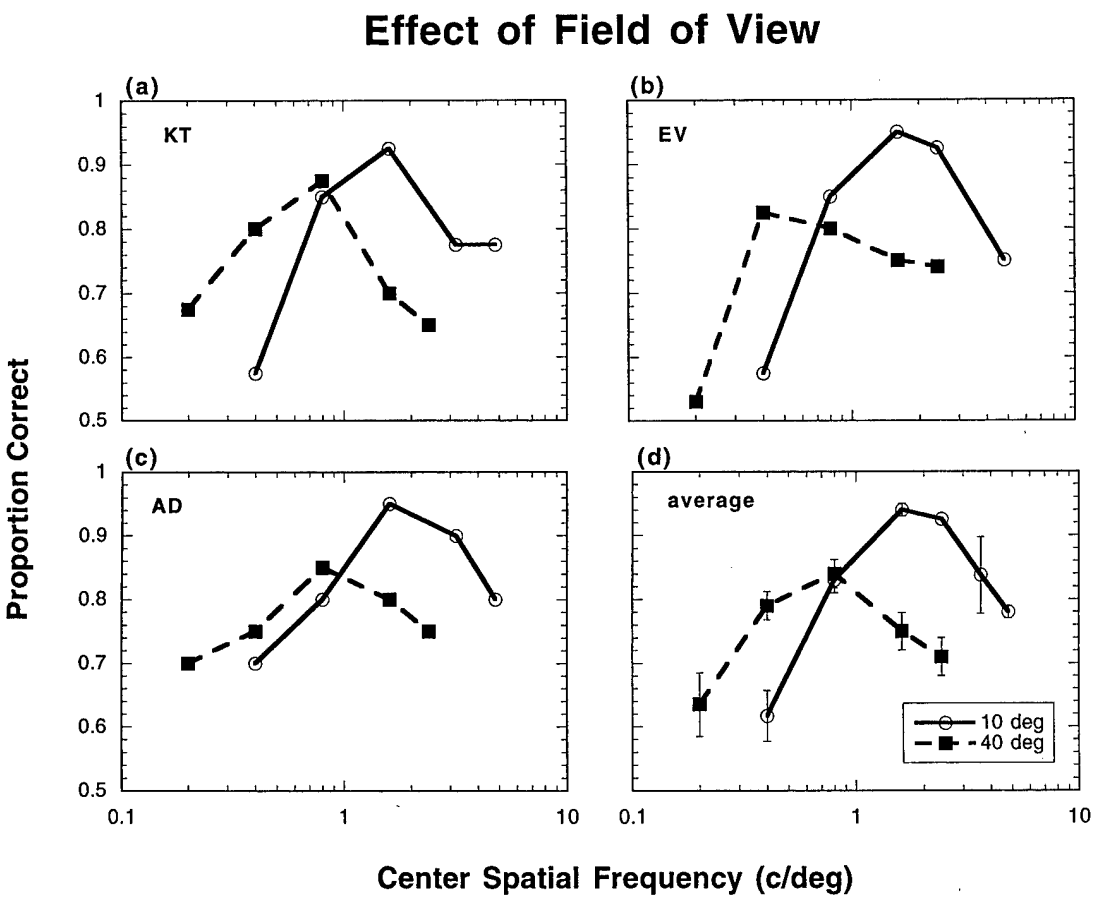

Fig. 8. Proportion of correct responses for direction discrimination plotted against the center spatial frequency of the optic flow patterns. Symbols represent data for optic flow patterns with fields of view of 10° × 10° (○) and 40° × 40° (■). Data shown are from subjects (a) KT; (b) EV; (c) AD: and (d) the mean across the three subjects. Error bars are ± 1 S.E.M.

5.1. Spatial frequency, temporal frequency, and speed

The trade-off between spatial frequency and speed implicates the role of temporal frequency in governing performance (spatial frequency × speed = temporal frequency). Previous studies with sinusoidal gratings have explored the temporal tuning of the visual motion system (Anderson & Burr, 1985; Wilson, 1985). The results support the existence of at least two temporal mechanisms: one bandpass with a peak around 10 Hz and the other lowpass (Anderson & Burr, 1985). The sensitivity of the filters depends on spatial frequency. Compared to the sensitivity of the low pass filter, the sensitivity of the bandpass filter is higher at low spatial frequencies and lower at high spatial frequencies. At intermediate spatial frequencies, the sensitivities of the two filters are equal (Hess & Snowden, 1992).

In Fig. 9, the data from Fig. 7d are replotted as a function of temporal frequency. The arrow on the upper X-axis marks the estimated peak of the hypothetical bandpass temporal filter (Anderson & Burr, 1985). Note that for the fastest optic flow speed the peak of the response curve is close to the estimated peak of the bandpass temporal filter. The slowest optic flow speed produced a consistently high response for the low temporal frequencies, which may be due to the contribution of the low pass temporal filter (Anderson & Burr, 1985). The response curve for the intermediate speed

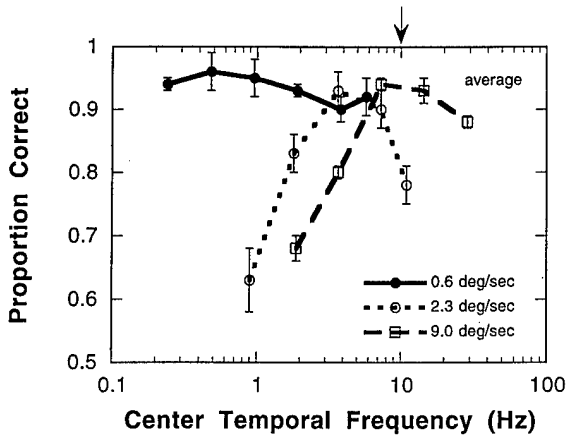

Fig. 9. Data of Fig. 7d replotted as a function of temporal frequency. The arrow on the upper X-axis marks the estimated peak of the hypothetical bandpass temporal filter.

pattern falls between these two curves, suggesting a contribution from both filters.

5.2. Limitations of the higher level motion mechanism imposed by the lower level

Anatomical and physiological studies have revealed a hierarchical organization of motion processing in the macaque monkey. Neurons in the striate cortex (V1) project directly to the middle temporal (MT) area of the superior temporal sulcus. Neurons in both V1 and MT respond to uniform motion in the fronto-parallel plane (Tanaka, Hikosaka, Saito, Yukie, Fukada & Iwai, 1986). MT neurons project to the medial superior temporal (MST) area of the superior temporal sulcus which also has a high proportion of directionally selective cells, and the neurons in the dorsal part of MST have been shown to respond selectively to radial or circular motion, with some responding to combinations of planar and radial and circular stimuli-components of optic flow (Tanaka, Fukada & Saito, 1989; Tanaka & Saito, 1989; Duffy & Wurtz, 1991; Orban et al., 1992; Duffy & Wurtz, 1995; Saito, Yukie, Tanaka, Hikosaka, Fukada & Iwai, 1986).

Several computational models have been proposed whereby the putative mechanism that processes optic flow (MSTd) is a linear integration of appropriately chosen MT units (Orban et al., 1992; Perrone, 1992; Verri et al., 1992; Lappe & Rauschecker, 1993; Perrone & Stone, 1994; Warren & Saunders, 1995). Recently Morrone, Burr and Vaina (1995) have provided psychophysical data to support the view that complex motion, such as radial and circular motion, is processed by a hierarchical motion system; an initial stage of motion processing by local motion mechanisms followed by an integration stage where the specialized mechanisms are tuned to complex motions. Morrone and colleagues showed that the contrast sensitivity for the detection of radial motion and the discrimination of the direction of radial motion are limited by the contrast threshold of the local motion detectors. In our study we show that the processing of the complex motion is also constrained by the spatial frequency tuning and the spatial frequency–speed interaction of the low level motion system. Together the two studies indicate that the higher level stage cannot enhance the limits imposed by the lower stages.

5.3. Implications of the findings for engineering applications

The results of this study have potential engineering applications. The current trend in simulations (e.g., flight simulators) is to reproduce the real world scene with high fidelity. The same principle is true for remote sensing devices or helmet mounted displays, where images are being transmitted. Transmitting high fidelity images is costly, and it may be that high fidelity is not necessary for accurate performance; information in the various spatial frequencies may not be necessary for the task at hand. Our study shows that for direction discrimination using optic flow, performance was not equivalent across all spatial frequencies. Information in some of the spatial frequencies did not allow for above chance discrimination performance. Given that a narrow band of spatial frequencies, optimally placed, is sufficient to support direction discrimination performance indicates that we can increase transmission efficiency without jeopardizing performance. It may be possible to filter images of real world scenes and transmit the information contained only in those spatial frequencies that are effective for successful performance. The reduced bandwidth for the transmitted information would translate into a savings in time without a cost in performance. The results of this study indicate that the choice of the optimal spatial frequency band will depend on the estimated mean image speed of the information to be transmitted. However, before the reported findings can be applied to engineering problems, it needs to be determined whether the results obtained with the random dot patterns generalize to optic flow patterns of real world scenes. The object structure of natural images may interact with spatial frequency for the discrimination of motion direction.

Acknowledgements

The authors thank Elisabeth Fine and three anonymous reviewers for helpful comments. J. Kim thanks Kyenghui Lee and Miru Kim for their encouragement. Effort sponsored by the Air Force Office of Scientific Research, Air Force Material Command, USAF, under grant number AFOSR-F49620-94-1-0187 to KAT. The U.S. Government is authorized to reproduce and distribute reprints for Governmental purposes notwithstanding any copyright notation thereon. The views and conclusions contained herein are those of the authors and should not be interpreted as necessarily representing the official policies or endorsements, either expressed or implied, of the Air Force Office of Scientific Research or the U.S. Government.

References

Anderson, S. J., & Burr, D. C. (1985). Spatial and temporal selectivity of the human motion detection system. *Vision Research, 25*, 1147–1154.

van den Berg, A. V. (1992). Robustness of perception of heading from optic flow. *Vision Research, 32*, 1285–1296.

Burr, D. C., & Ross, J. (1982). Contrast sensitivity at high velocities. *Vision Research, 22*, 479–484.

Crowell, J. A., & Banks, M. S. (1993). Perceiving heading with different retinal regions and types of optic flow. *Perception and Psychophysics, 53*, 325–337.

Cutting, J. E. (1986). *Perception with an eye for motion*. Cambridge, MA: MIT.

Duffy, C. J., & Wurtz, R. H. (1991). Sensitivity of MST neurons to optic flow stimuli. II. Mechanisms of response selectivity revealed by small-field stimuli. *Journal of Neurophysiology, 65*, 1346–1359.

Duffy, C. J., & Wurtz, R. H. (1995). Response of monkey MST neurons to optic flow stimuli with shifted centers of motion. *Journal of Neuroscience, 15*, 5192–5208.

Duffy, C. J., & Wurtz, R. H. (1997). Medial superior temporal area neurons respond to speed patterns in optic flow. *Journal of Neuroscience, 17*, 2839–2851.

Gibson, J. J. (1950). *Perception of the visual world*. Boston, MA: Houghton Mifflin.

Hess, R. F., & Snowden, R. J. (1992). Temporal properties of human visual filters: number, shapes and spatial covariation. *Vision Research, 32*, 47–50.

Kelly, D. H. (1979). Motion and vision. II. Stabilized spatio-temporal threshold surface. *Journal of the Optical Society of America A, 69*, 1340–1349.

Lappe, M., & Rauschecker, J. P. (1993). A neural network for the processing of optic flow from ego-motion in higher mammals. *Neural Computation, 5*, 374–391.

Morrone, M. C., Burr, D. C., & Vaina, L. M. (1995). Two stages of visual processing for radial and circular motion. *Nature, 376*, 507–509.

Nakayama, K., & Tyler, C. W. (1981). Psychophysical isolation of movement sensitivity by removal of familiar position cues. *Vision Research, 21*, 427–433.

Orban, G. A., Laae, L., Verri, A., Raiguel, S., Xiao, D., Maes, H., & Torre, V. (1992). First-order analysis of optical flow in monkey brain. *Proceedings of the National Academy of Science USA, 89*, 2595–2599.

Pelli, D., & Zhang, L. (1991). Accurate control of contrast on microcomputer displays. *Vision Research, 31*, 1337–1350.

Perrone, J. A. (1992). Model for the computation of self-motion in biological systems. *Journal of the Optical Society of America A, 9*, 177–194.

Perrone, J. A., & Stone, L. S. (1994). A model of self-motion estimation within primate extrastriate visual cortex. *Vision Research, 34*, 2917–2938.

Riemersma, J. B. J. (1981). Visual control during straight road driving. *Acta Psychologia, 48*, 215–225.

Royden, C. S., Banks, M. S., & Crowell, J. A. (1992). The perception of heading during eye movements. *Nature, 360*, 583–585.

Royden, C. S., Crowell, J. A., & Banks, M. S. (1994). Estimating heading during eye movements. *Vision Research, 34*, 3197–3214.

Saito, H., Yukie, M., Tanaka, K., Hikosaka, K., Fukada, Y., & Iwai, E. (1986). Integration of direction signals of image motion in the superior temporal sulcus of the macaque monkey. *Journal of Neuroscience, 6*, 145–157.

Sekuler, A. (1991). Speed discrimination in looming displays: critical elements of motion and integration. Unpublished Doctoral Dissertation, University of California, Berkeley.

Tanaka, K., Fukada, Y., & Saito, H. A. (1989). Underlying mechanisms of the response specificity of expansion/contraction and rotation cells in the dorsal part of the medial superior temporal area of the macaque monkey. *Journal of Neurophysiology, 62*, 642–656.

Tanaka, K., Hikosaka, K., Saito, H., Yukie, M., Fukada, Y., & Iwai, E. (1986). Analysis of local and wide-field movements in the superior temporal visual areas of the macaque monkey. *Journal of Neuroscience, 6*, 134–144.

Tanaka, K., & Saito, H. (1989). Analysis of motion of the visual field by direction, expansion/contraction, and rotation cells clustered in the dorsal part of the medial superior temporal area of the macaque monkey. *Journal of Neurophysiology, 62*, 626–641.

Turano, K., & Wang, X. (1994). Visual discrimination between a curved and straight path of self motion: effects of forward speed. *Vision Research, 34*, 107–114.

Turano, K. A. (1995). Self-motion path discrimination: effects of image stabilization. *Journal of Vestibular Research, 5*, 411–420.

Verri, A., Straforini, M., & Torre, V. (1992). A model of spatial organisation of the receptive fields of neurons in the middle superior temporal area. *Perception (Supplement, 2), 21*, 64.

Warren, W. H., & Hannon, D. J. (1988). Direction of self-motion is perceived from optical flow. *Nature, 336*, 162–163.

Warren, W. H., Morris, M. W., & Kalish, M. (1988). Perception of translational heading from optical flow. *Journal of Experimental Psychology (Human Perception and Performance), 14*, 646–660.

Warren, W. H., & Saunders, J. A. (1995). Perceiving heading in the presence of moving objects. *Perception, 24*, 315–331.

Warren, W. H. J., & Hannon, D. J. (1990). Eye movements and optical flow. *Journal of the Optical Society of America A, 7*, 160–169.

Warren, W. H. J., Mestre, D. R., Blackwell, A. W., & Morris, M. W. (1991). Perception of circular heading from optical flow. *Journal of Experimental Psychology (Human Perception and Performance), 17*, 28–43.

Watamaniuk, S. N., & Duchon, A. (1992). The human visual system averages speed information. *Vision Research, 32*, 931–941.

Watson, A. B., & Turano, K. (1995). The optimal motion stimulus. *Vision Research, 35*, 325–336.

Weibull, W. (1951). A statistical distribution function of wide applicability. *Journal of Applied Mechanics, 18*, 292–297.

Wilson, H. R. (1985). A model for direction selectivity in threshold motion perception. *Biological Cybernetics, 51*, 213–222.

PERGAMON

Vision Research 39 (1999) 1177–1187

Vision Research

Eye movements affect the perceived speed of visual motion

Kathleen A. Turano [a,*], Susan M. Heidenreich [b]

[a] *The Johns Hopkins University School of Medicine, Wilmer Eye Institute, Baltimore, MD, USA*
[b] *University of San Francisco, San Francisco, CA, USA*

Received 23 April 1997; received in revised form 6 May 1998

Abstract

Eye movements add a constant displacement to the visual scene, altering the retinal-image velocity. Therefore, in order to recover the real world motion, eye-movement effects must be compensated. If full compensation occurs, the perceived speed of a moving object should be the same regardless of whether the eye is stationary or moving. Using a pursue-fixate procedure in a perceptual matching paradigm, we found that eye movements systematically bias the perceived speed of the distal stimulus, indicating a lack of compensation. Speed judgments depended on the interaction between the distal stimulus size and the eye velocity relative to the distal stimulus motion. When the eyes and distal stimulus moved in the same direction, speed judgments of the distal stimulus approximately matched its retinal-image motion. When the eyes and distal stimulus moved in the opposite direction, speed judgments depended on the stimulus size. For small sizes, perceived speed was typically overestimated. For large sizes, perceived speed was underestimated. Results are explained in terms of retinal-extraretinal interactions and correlate with recent neurophysiological findings.

Keywords: Speed perception; Eye movements; Retinal-image motion; Smooth pursuit eye movements; Motion perception

1. Introduction

Within our field of view, objects move in various directions at various speeds. Depending upon the saliency of the visual information and the task at hand, our eyes pursue or track one of the many moving objects. In doing so, the motion of that object, as well as the motion of the other moving objects, and the visual scene in general, are altered in the image on our retinas. Smooth pursuit eye movements add a velocity field to the visual scene that determines the velocity of the retinal motion. That is, the motion vectors for the distal stimulus and the eye-movement are added [illustrated in Fig. 1 of Turano & Heidenreich (1996)].

One important question is whether smooth pursuit eye movements affect speed perception in a manner consistent with the transformed retinal speed. We have previously shown that speed discrimination performance varies with the eye motion relative to the distal motion. Although discrimination measures indicate the precision of performance, they do not reveal whether the percept of the moving distal stimulus is systematically biased in a particular fashion. In the present study, we determined how the perceived speed of a distal stimulus changes as a function of the speed and direction of the eye movement relative to the motion of the distal stimulus.

Several studies have investigated the effects of eye movements on object motion perception (Wertheim, 1981; Pola & Wyatt, 1989; Brenner & van den Berg, 1994; Wertheim, 1994) and self-motion perception (Warren & Hannon, 1990; Royden, Banks & Crowell, 1992; Royden, Crowell & Banks, 1994; Freeman, Crowell & Banks, 1996) and have reached various conclusions. Some studies have concluded that eye movements do not affect the perception of distal motion (Warren & Hannon, 1990; Royden, Banks & Crowell, 1992; Royden, Crowell & Banks, 1994), whereas other studies have demonstrated that, at least in some situations, eye movements do affect distal motion perception (Wertheim, 1981; Pola & Wyatt, 1989; Brenner & van den Berg, 1994; Wertheim, 1994; Freeman, Crowell & Banks, 1996; Turano & Heidenreich, 1996).

* Corresponding author. Present address: Lions Vision Center, 550 North Broadway, 6th floor, Baltimore, MD 21205, USA. Tel.: +1 410 5026434; fax: +1 410 9551829; e-mail: kathy@lions.med.jhu.edu

0042-6989/99/$ - see front matter
PII: S0042-6989(98)00174-6

One prevailing view is that the perception of distal motion is based on an internal representation that consists of retinal and extraretinal signals (Wertheim, 1981; Pola & Wyatt, 1989; Brenner & van den Berg, 1994; Wertheim, 1994; Turano & Heidenreich, 1996). However, other findings suggest that under certain conditions, the only information used to judge distal motion is the retinal-image motion (Brenner & van den Berg, 1994; Turano & Heidenreich, 1996). We (Turano & Heidenreich, 1996) found that changes in retinal-image motion due to eye movements can account for the elevated speed-discrimination thresholds, except when the eyes move faster than the distal stimulus. In that case, speed-discrimination thresholds are higher than predicted on retinal-image motion alone indicating that some factor other than retinal-image motion is involved.

In this study we test the distal-motion model and the retinal-motion model in a speed-matching experiment to determine how the perceived speed of a distal stimulus changes as a function of the speed and direction of eye movements. The distal-motion model assumes that the effects of eye movements can be fully compensated, and therefore the perceived motion of a stimulus should be the same whether the eye is stationary or moving. According to this model, perceived speed, P, obeys a vector summation rule of the retinal, S_R, and extraretinal, S_{eye}, signals (Eq. (1)).

$$P = \sqrt{S_R^2 + S_{eye}^2 + 2\cos\theta\, S_R S_{eye}} \quad (1)$$

When the angle, θ, between the retinal and the extraretinal signals is 0, Eq. (1) reduces to

$$P = S_R + S_{eye} \quad (2)$$

and when the angle is 180°, Eq. (1) reduces to

$$P = |S_R - S_{eye}|. \quad (3)$$

In contrast, the retinal-motion model assumes that there is no compensation for the retinal effects of the eye movements, and therefore observers should make perceptual judgments of the real-world motion only on the basis of the retinal-image motion.

We investigated whether the perceived speed of a moving stimulus viewed with a moving eye is the same as the perceived speed of the same stimulus viewed with a stationary eye. We used a perceptual-matching task to estimate a threshold point on the psychometric function that anchors the function (i.e. the point of subjective equality); this differs from discrimination measures that reflect the slope of the psychometric function and only provide an estimate of the precision of the judgments. In effect, the perceptual-matching threshold indicates the speed of a test stimulus viewed while making pursuit eye movements that appears to be equal to the speed of a reference stimulus viewed while fixating a stationary point.

2. General method

2.1. Pursue-fixate procedure

Perceptual matches were determined using a pursue-fixate procedure in a perceptual matching paradigm, illustrated in Fig. 1. On each trial, the subject was presented with two motion sequences of a translating distal stimulus. In the first motion sequence, the stimulus moved at a test speed (reference speed $\pm\Delta$ speed). In the second motion sequence, the stimulus always moved at the reference speed. The subject's task was to indicate in which of the two motion sequences the stimulus moved faster. No feedback was given.

To test the interaction of eye and distal stimulus motion, the subject was instructed to pursue (or track) a translating pursuit target during the presentation of the first sequence until the distal stimulus disappeared and then to fixate the centrally-located stationary point during the presentation of the second sequence. By keeping the eye relatively still during the presentation of the distal stimulus moving at the reference speed, the end result is an estimate of the perceived motion of the stimulus during eye movements relative to the same stimulus viewed with a stationary eye. A brief interval (2 s) between the two motion sequences allowed the subject to switch from pursue to fixate. A tone indicated the start of each trial. The time between trials was approximately 3.5 s.

2.2. Staircase procedure

Two independent interleaved staircases were used; one was initiated from the negative side ($-\Delta$ speed) and the other was initiated from the positive side ($+\Delta$ speed). On each trial, one of the two staircases was randomly chosen, designating the Δ speed based on the subject's previous response for that staircase. After a single correct judgment, the Δ was decreased by half and after one incorrect response, the Δ was increased in a similar manner, with a minimum delta set at 0.05 °/s. The procedure was such that the two interleaved staircases could potentially cross and recross (Cornsweet, 1962). The test session ended after ten reversals per staircase, requiring approximately 50 trials per session. Speed match error was computed as the mean of all the Δ speed (for both staircases) presented after the data collection began (Fendick, 1985). Response variability was calculated as half the difference between the independently calculated signed means of the two staircase Δ speeds (Fendick, 1985).

2.3. Eye-movement recording

We followed the same procedure used previously to record eye movements (Turano & Heidenreich, 1996).

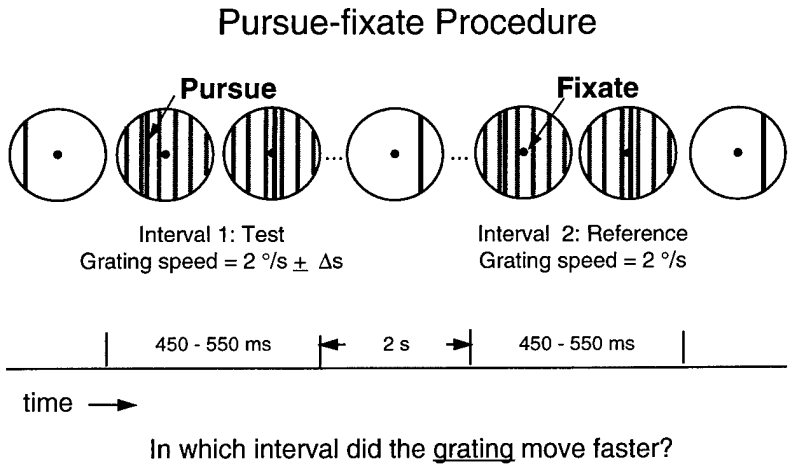

Fig. 1. Illustration of the time course for the pursue-fixate procedure. The dark bar represents the pursuit target and the grating represents the distal stimulus. The grating was presented twice in succession. Subjects were instructed to pursue the bar until the grating disappeared and then to fixate a centrally-positioned stationary point during the second interval. The bar and fixation point were visible throughout the experimental session. The subjects' task was to indicate in which interval the grating moved faster.

Because accurate eye-movement records are critical to our evaluation of the models, the procedure is described again here. Eye velocity was measured throughout each trial using an SRI Generation-V dual Purkinje-image eyetracker (Crane & Steele, 1985). The subject viewed the display with the right eye and wore an opaque patch over the left eye. The head was stabilized with a bite bar and headrest. Eye velocity for the right eye was determined from the voltage analogs of horizontal eye position. The voltages were fed into an analog-to-digital converter every 10 ms and stored on a computer for off-line analysis. Voltage was converted to degrees of visual angle, on the basis of each subject's calibration results. The calibration procedure was as follows: 25 equally spaced points, extending 6° horizontally and vertically, were displayed in sequence on a CRT display screen positioned 2 m in front of the subject. To calibrate each position, a dot appeared at the center of the monitor and the subject pushed a button when she or he was fixating the dot. The central dot then disappeared, and a calibration dot appeared. The subject fixated that dot, and the voltage and screen position were recorded. To convert voltage to degrees of visual angle, a regression line was fit to the dots' horizontal positions, expressed in terms of visual angle, plotted against the horizontal positions of the eye, expressed in terms of voltage.

2.4. Eye-movement analysis

Average horizontal eye velocity was computed as the slope of horizontal eye position over time and was determined separately for the pursuit and fixation intervals of each trial. Prior to calculating pursuit eye velocity, saccadic eye movements were identified and eliminated in the following manner: A threshold velocity was set at 14 °/s. If the eye velocity between any two successive samples exceeded the threshold, those two and the next four samples were excluded from the analysis. For motion sequences in which samples were removed, eye velocity was defined as the average, weighted by the number of samples, of the separately-computed slopes for the individual segments.

3. Experiment 1: speed matching of optimal distal speed

3.1. Methods

The stimuli were generated by a graphics display board (Cambridge Research Systems), controlled by an IBM-compatible AT computer, and displayed on a Joyce DM2 monitor with a refresh rate of 100 Hz. The display screen was masked with a circular aperture that was 8° in diameter. Viewing distance was 2 m. The parameters of the distal stimulus were chosen to stimulate the most efficient motion sensor (Watson & Turano, 1995). The stimulus was a vertically-oriented, 3-c/° sine-wave grating, moving at a reference speed of 2.0 °/s. The contrast of the grating was 20%.

A vertical bar (0.06° wide, 10% positive contrast) that served as the pursuit target moved across the display screen at a specified velocity and was continuously present throughout the experimental session. The bar's speed (0–4 °/s) and direction (same or opposite to the grating) were the same within a block of trials and randomly manipulated across blocks. The pursuit target moved across the display screen at a constant velocity and wrapped around when it reached the edge. The pursuit target and stimulus velocities were independent of each other. The fixation point was a black

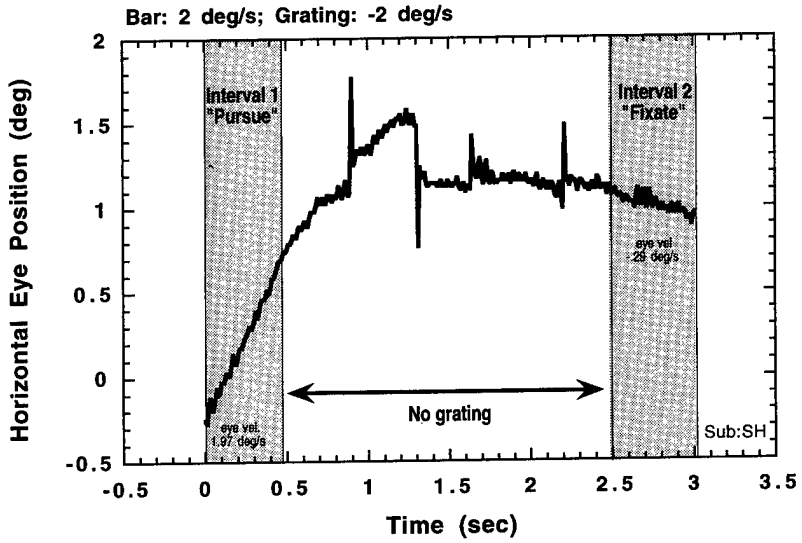

Fig. 2. Horizontal eye position plotted against time. Average eye velocity, computed as the slope of eye position over time, was determined separately for the "pursue" and the "fixate" intervals. Data from one trial in Experiment 1; distal grating velocity = −2°/s; pursuit target velocity = 2°/s, "pursue" interval eye velocity = 1.97°/s; "fixate" interval eye velocity = −0. 29°/s.

opaque circle (0.2° diameter) which remained taped on the display screen at its central position.

The duration of each of the two motion sequences within a trial was randomly chosen from a Gaussian distribution centered at 500 ms (S.D. = 50 ms). The stimuli in the two motion sequences always moved in the same direction, right or left, and the direction of motion remained fixed throughout each experimental session. The direction of grating motion was systematically alternated across sessions.

Three observers (including the two authors) with normal or corrected-to-normal acuities, well trained in the pursue-fixate procedure, served as subjects.

3.2. Results

Fig. 2 is the eye-movement record of one trial. Horizontal eye position is plotted against time. The two shaded areas represent the intervals in which the two motion sequences were presented. During the first motion sequence the subject was instructed to pursue the bar until the grating disappeared and then to fixate the stationary mark throughout the period of the second motion sequence. In the time period between the two intervals there was no grating pattern on the screen. The eye positions presented in Fig. 2 are from a trial in which the pursuit target moved rightward at a speed of 2 °/s and the reference stimulus moved leftward at a speed of 2 °/s. During the first interval the eye moved rightward at a speed of 1.97 °/s and during the second interval the eye moved leftward at 0.29 °/s.

Subjects were able not only to switch from pursuit to fixation during the 2-s time interval, but they were also able to keep their eyes fairly stable during the second interval. The average eye velocities measured during interval 2 ("fixate") are 0.21 °/s (S.D. = 0.14) for subject FT, 0.41 °/s (S.D. = 0.22) for subject SH, and 0.16 °/s (S.D. = 0.07) for subject KT.

In Fig. 3, we plot the speed of the test grating that appears equal to the speed of the reference speed (i.e. speed match) as a function of the eye velocity. According to the retinal-motion model (prediction shown as solid line in Fig. 3), speed match should vary in proportion to eye velocity because, to equate the perceived speeds of the reference and test gratings, the speed of the test grating needs to be adjusted by an amount equivalent to the eye velocity. According to the distal-motion model (prediction shown as dashed line in Fig. 3), speed match should equal the reference speed regardless of the eye velocity.

The symbols in Fig. 3 represent the three subjects' speed match data. The eye velocity is the mean eye velocity calculated during the first interval, averaged over all the trials in a session. The horizontal error bars on each data point indicate the standard deviation of the eye velocities for that test session. The mean gains (i.e. eye speed divided by pursuit target speed) were 0.67 (S.D. = 0.21), 0.88 (S.D. = 0.15), and 0.74 (S.D. = 0.28) for subjects FT, KT, and SH, respectively.

The speed match data cannot be fully explained by either of the two models. For eye movements in the same direction as the distal stimulus (unshaded area in Fig. 3), the speed matches fall between the predictions of the retinal-image and distal motion models. For eye movements in the opposite direction to the distal stimulus, the data of two subjects approximate the prediction of a distal motion model and the data of the third subject fall between the predictions of the distal-motion and retinal-motion models.

3.3. Discussion

The results of Experiment 1 demonstrate that eye movements can affect the perceived speed of distal-stimuli. An eye movement of only 1°/s in the same direction as a 2°/s distal stimulus can decrease its perceived speed by as much as 25% of its speed (0.5°/s), when compared to its perceived speed when viewed with a stationary eye. However, the effects of eye movements on the perceived speed of distal-stimuli are not determined by eye speed alone. The results show an asymmetry in the speed match errors with respect to the relative direction of eye and distal motion. An eye movement of 1.5°/s in the opposite direction of the distal motion produces a speed match error less than 0.3°/s, whereas a 1.5°/s eye movement in the same direction produces an error greater than 1°/s.

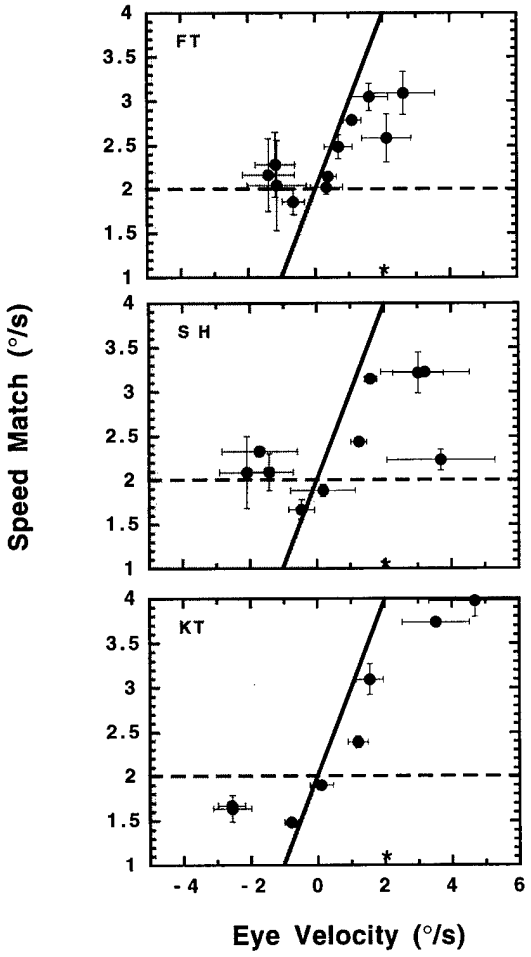

Fig. 3. Speed match plotted as a function of actual eye velocity. Positive and negative values of eye velocity indicate movement in the same and opposite direction as the grating, respectively. The predicted match for the retinal-motion model is shown as a solid diagonal line. The predicted match for the distal-motion model is shown as a broken horizontal line at 2.0°/s. Shaded area, eye movement in the opposite direction to the distal stimulus motion; unshaded area, eye movement in the same direction as the distal stimulus motion. Error bars represent ± 1 S.D. Stars indicate the velocity of the reference distal stimulus (2°/s). Data are for subjects FT (a), SH (b), and KT (c).

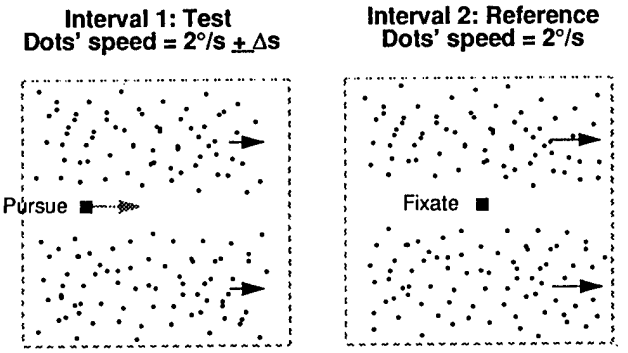

Fig. 4. Illustration of the display in the pursue and fixates phases in Experiment 2. The distal stimulus was an array of randomly positioned dots that moved horizontally within a stationary window. A single square, positioned within a horizontal gap that divided the window, served as both the pursuit target (in the pursue phase) and the stationary fixation point (in the fixate phase). The dashed box outlining the window is for illustration purpose only; it was not present in the display.

It is possible that the spatial superposition of the pursuit target (as well as fixation point) and the grating would excite local relative motion detectors; this in turn may have affected the perceived speed of the grating. In the next experiment, we modified the display to eliminate the spatial superposition and re-examined the subjects' judgments using the same pursue-fixate task.

4. Experiment 2: effect of non-overlapping pursuit target and grating

4.1. Methods

The stimuli were generated by a Silicon Graphics OCTANE workstation and displayed on a Silicon Graphics Color Graphics Display (Model GDM 20E21) with a refresh rate of 72 Hz. Viewing distance was 0.57 m. The distal stimulus was an array of randomly positioned dots (density of 1 dot/deg^2) that moved horizontally within a stationary 8 × 8° window. Each dot was composed of a 3 × 3 pixel array (0.09 × 0.09°) and had a luminance of 28.5 cd/m^2. A single square (5 × 5 pixel array—0.15 × 0.15°, 28.5 cd/m^2), positioned within a horizontal gap (2.5°) that divided the window, served as both the pursuit target (in the pursue phase) and the stationary fixation point (in the fixate phase). Fig. 4 illustrates the display in the pursue and fixate phases.

A trial proceeded as follows: The display screen was uniformly illuminated at 5.3 cd/m^2 for the first 0.1 s. Next, the pursuit target appeared and traversed horizontally within the gap at a specified velocity for a total

of 1.5 s. When the pursuit target had been presented for 1 s, the dots appeared and moved within the window for 0.5 s. The dots and pursuit target disappeared, and the screen was again uniformly illuminated for 1 s. The fixation point then appeared centered within the gap and remained stationary for 1.5 s. During the last 0.5 s of fixation the dots appeared and moved within the window at the reference velocity of 2.0°/s. The two authors served as subjects.

4.2. Results

In Fig. 5, we plot speed matches as a function of eye velocity, using the same plotting conventions as in Fig. 3. Solid symbols represent the data of Experiment 1, replotted for comparison purposes. The open symbols represent the data obtained with the display using the non-overlapping pursuit target and distal stimulus.

For eye movement in the same direction as the distal stimulus, the general trend in speed match as a function of eye velocity was the same regardless of the display type; performance was the same when the pursuit target (and fixation point) were superimposed on the distal stimulus and whether the distal stimulus was a grating or an array of randomly positioned points.

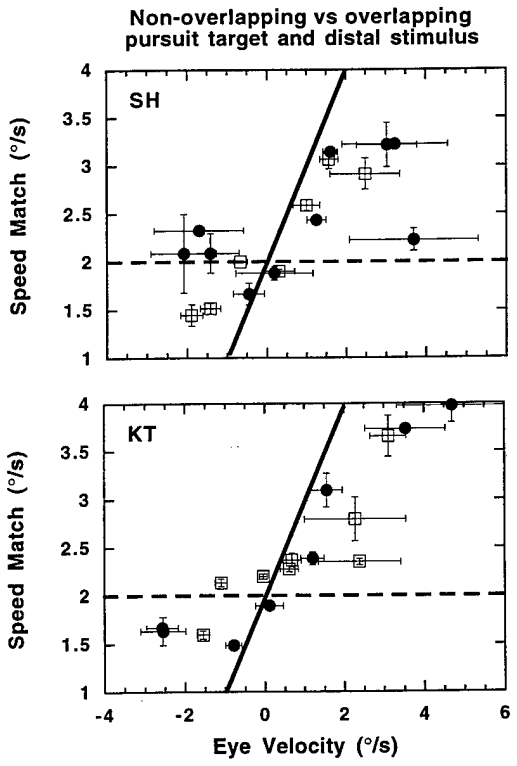

Fig. 5. Speed match plotted as a function of eye velocity, using the same plotting conventions as in Fig. 3. Solid symbols represent the data of Experiment 1, replotted from Fig. 3 for comparison purposes. The open symbols represent data obtained with the display using the non-overlapping pursuit target and distal stimulus.

The distal stimulus was perceived to move more slowly when the eye moved in the same direction than when the eye was stationary. However, with the modified display, when the eye moved in a direction opposite the distal stimulus it was perceived more often to move slightly faster than when the eye was stationary.

In our pursue-fixate procedure, not only did the retinal motion of the distal stimulus differ between the pursue and fixate intervals, but so did the retinal motion of the stimulus aperture. The relative motion of the grating and aperture may have affected the perceived speed of the distal stimulus. In the first two experiments, the display window subtended a relatively small visual angle (8 × 8°) which may have increased the salience of the relative motion of the grating and aperture. To test whether stimulus size had an impact on the estimated distal stimulus speed, we repeated the procedure with a larger display. In addition, we tested the generalizability of the effect using additional reference speeds.

5. Experiment 3: effects of display size and reference speed

5.1. Methods

The methods were the same as described in Experiment 2 with the exception that speed matches were determined for three reference speeds (2.0, 4.0, and 6.0°/s) for each of two window sizes (38 × 28° and 8 × 8°).

5.2. Results

Fig. 6 plots the speed matches obtained with the large (38 × 28°, solid symbols) and small displays (8 × 8°, open symbols) for the three different reference speeds for subjects SH and KT. Plotting conventions are the same as described for Fig. 3. Table 1 lists the mean pursuit gains of the two subjects for the various conditions. Note that there is little difference between the mean gains for the large and small stimulus sizes and for the stimulus speeds.

The most striking difference between the datasets for the large and small stimulus displays is the difference in the perceived speed of the distal stimulus when the eye moves in the opposite direction (indicated on the x-axis by the negative eye velocities). With the larger stimulus, when moving their eyes subjects chose a faster distal stimulus as a perceptual match, indicating that they perceived the distal stimulus to be moving slower during pursuit eye movements than when the eye was stationary. With the

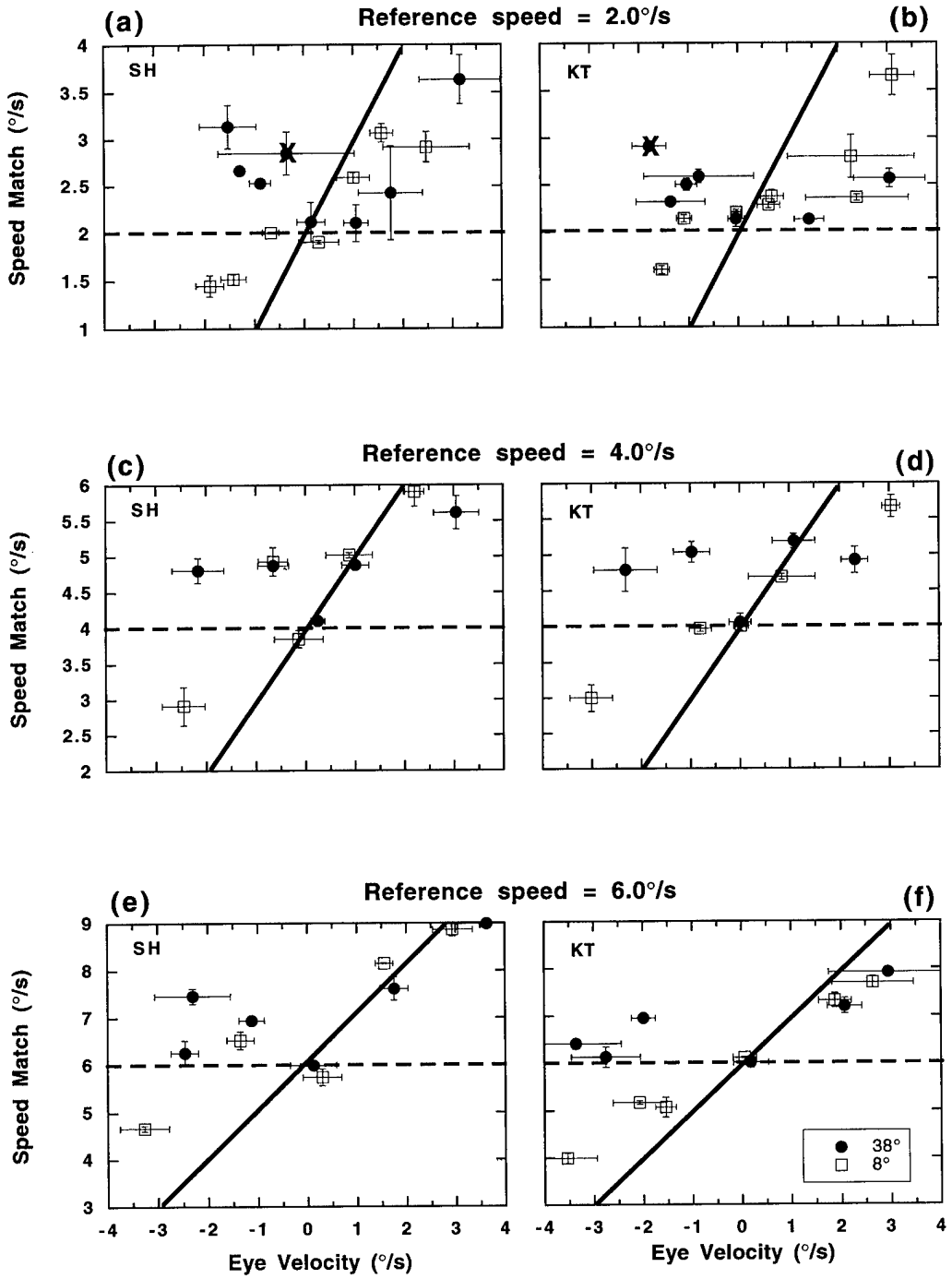

Fig. 6. Speed match plotted as a function of eye velocity obtained with the large (38 × 28°, solid symbols) and small displays (8 × 8°, open symbols). Data for the three different reference speeds are shown in separate graphs: 2.0°/s (a, b), 4.0°/s (c, d), and 6.0°/s (e, f), for subjects SH and KT, respectively. The symbols denoted by an X in a and b represent data obtained with a 38 × 28° display with an opaque border outlining a square (8 × 8°) superimposed. The reference speed was 2.0°/s and eye velocity was −2.0°/s. Plotting conventions are the same as described for Fig. 3.

small stimulus, however, the subjects generally perceived the distal stimulus to be moving faster than when the eye was stationary; this effect occurred with all three reference speeds. Thus, the size of the distal stimulus had a significant effect on the perceived speed of the distal-stimuli when the eye moved in the opposite direction to the distal stimulus.

The pattern of results was different, however, when the eye moved in the same direction as the distal stimulus. There was little difference in the

Table 1
Mean values and S.D. of eye velocity-to-pursuit target gain

Stimulus speed (°/s)	Stimulus size (°)	Subject			
		KT		SH	
		Mean	S.D.	Mean	S.D.
2.0	8	0.69	0.24	0.79	0.15
2.0	38	0.72	0.23	0.83	0.14
4.0	8	0.92	0.11	0.77	0.10
4.0	38	0.90	0.16	0.85	0.19
6.0	8	0.86	0.15	0.75	0.06
6.0	38	0.86	0.15	0.71	0.17

speed matches obtained with the large and small windows. The distal stimulus was perceived to be moving more slowly than when the eye was stationary. Again, the effect was replicated across all three reference speeds.

5.3. Discussion

The results of Experiment 3 suggest that when the eye moves in the opposite direction to the distal stimulus the display size plays a role in determining perceived speed. To ascertain whether the size of the display, per se, was a critical factor or whether the critical factor was the location of motion signals generated at the window boundaries, subjects repeated a session (pursuit target velocity -2°/s, window size 38×28°) with a superimposed opaque border (1° wide black masking tape) outlining a square (8×8°) positioned at the center of the display. These black edges would have generated motion signals at the same spatial location as the motion signals at the boundaries in the small display condition. The results for this manipulation are indicated by an X in Fig. 6a,b. The data show that the perceived speed of the distal stimulus is not affected by the absence or presence of boundaries in the near periphery.

To more fully map the function of perceived speed versus stimulus size at a particular pursuit velocity (-2°/s), subjects participated in two ancillary sessions. The experimental methods of the ancillary sessions were the same as described in Experiment 2 with the exception that the window sizes were 12° in one session and 18° in the other. Fig. 7 plots speed match as a function of window size. The horizontal line at 2°/s indicates an equivalent match in perceived speed between the moving-eye and stationary eye viewing conditions. The graph shows that the perceived speed of a distal stimulus varies in a systematic manner with stimulus size. For a small stimulus (8°), eye movements in the opposite direction to the stimulus serve to increase the perceived speed of the stimulus. For stimulus sizes of 18° and greater, eye movements in the opposite direction to the stimulus serve to decrease the perceived speed of the stimulus.

6. General discussion

The results of this study demonstrate that, in general, eye movements affect the perceived speed of a distal stimulus. We find no evidence to support the distal-motion model. We have identified an interaction between two factors that influence the eye-movement effect on perceived speed. One factor is the direction of the eye-movement relative to the distal stimulus motion, and the other factor is the size of the distal stimulus.

When a person's eyes move in the same direction as a distal stimulus, it appears slower than when the person's eyes are still. Under these conditions, speed judgments are relatively close to the predictions generated by the retinal-motion model particularly for the faster reference speeds; the effects of eye movements on the retinal-image motion are not compensated. For the stimulus parameters that we tested, an extra-retinal

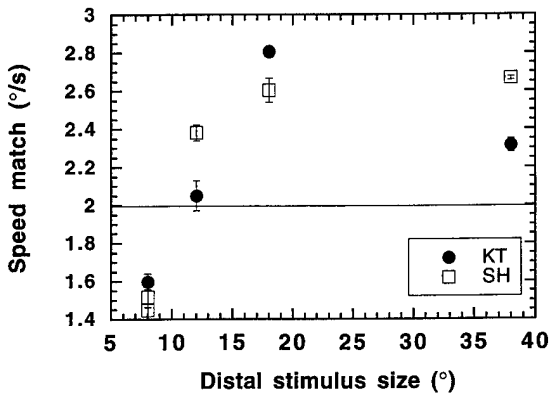

Fig. 7. Speed match plotted as a function of stimulus display width at a pursuit velocity of -2.0°/s for subjects KT (solid symbols) and SH (open symbols). The horizontal line at 2°/s indicates an equivalent match between the moving-eye and stationary-eye viewing conditions. Data for the 8 and 38° sizes were obtained in Experiment 3 (reference speed, 2.0°/s; pursuit velocity, -2.0°/s), replotted from Fig. 6.

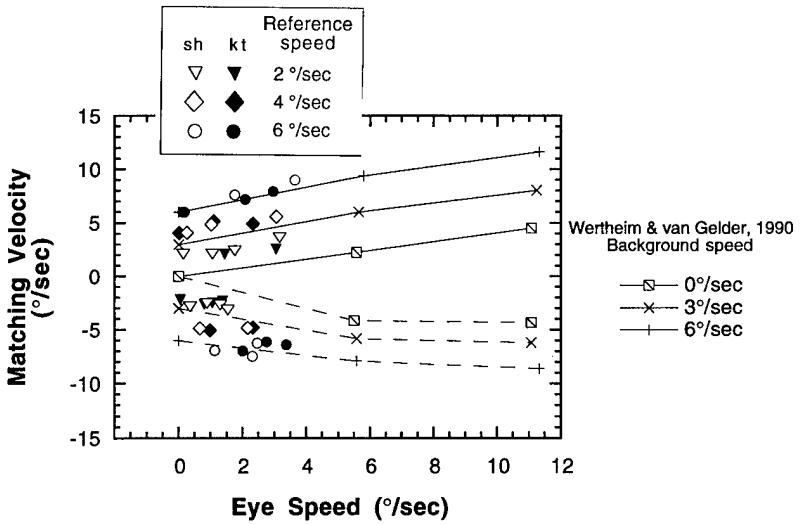

Fig. 8. Speed match data plotted as a function of eye speed. The speed match data (for the 38° display size) from Fig. 6 of the present paper are plotted together with a subset of the data from Wertheim & van Gelder (1990). The solid and dashed lines connect symbols for the same and opposite directions of eye and background motion, respectively, of the Wertheim and van Gelder study. Different symbols represent different background speeds.

signal does not appear to contribute significantly to the distal stimulus speed judgments.

When a person's eyes move in the opposite direction to a distal stimulus, its perceived speed depends on its size. When the stimulus is small ($< \sim 12°$) most judgments fall between a retinal-image match and a distal stimulus match. Data falling between the two could be accounted for by the contribution of an extra-retinal signal that under-represents eye velocity. The idea that the extra-retinal signal could under-represent eye velocity has been purported by several researchers (Gibson, Smith, Steinschneider & Johnson, 1957; Mack & Herman, 1973; Wertheim, 1987) and demonstrated by the Aubert-Fleischl phenomenon (i.e. a pursued stimulus appears slower than the same stimulus viewed with a stationary eye). When the stimulus is large, however, the judgments indicate that the perceived speed is underestimated. This could be explained by the contribution of an extra-retinal signal that over-represents eye velocity (i.e. the extra-retinal signal amplifies or over-estimates the speed of the eye).

6.1. Possible neurophysiological correlates

The idea that the extra-retinal signal could over-represent the eye velocity has some support from recent neurophysiological studies by Komatsu & Wurtz (1988). Recordings were made of cells located in the medial superior temporal (MST) area of the monkey cortex that have both an extra-retinal input and a visual response input. Some of these "pursuit" cells responded preferentially to small stimulus displays and others to large stimulus displays. The firing rate of many of the cells that responded preferentially to the large stimulus displays was greater when there was retinal motion of the background in the opposite direction to the pursuit than when pursuit was in the dark. The retinal motion served to increase the output of the pursuit cells. This was not the case when the preferred direction of stimulus motion and pursuit was the same. In this situation, interaction between the pursuit-related response and the visual stimulation was highly variable.

In the same study, Komatsu and Wurtz demonstrated that the pursuit cells that responded preferentially to the large stimulus displays showed a reversal in preferred direction as the stimulus size increased. This response change indicates that for some MST cells display size plays a role in modulating the retinal-extraretinal interaction (Komatsu & Wurtz, 1988).

6.2. Relation to other psychophysical studies

Using a speed magnitude estimation procedure and a $60 \times 20°$ display, Wertheim & van Gelder (1990) showed that the speed of the background pattern was underestimated when the eyes moved in the same direction as the background and, for background speeds slower than 9°/s, when the eyes moved in the opposite direction to the background. At a faster background speed, it was no longer underestimated. In our study we only investigated stimulus speeds of up to 6°/s. At these speeds, our results with the large stimulus display are comparable to theirs; background (stimulus) speed is underestimated during pursuit eye movements. In order to more directly compare the results of the two studies, we have replotted a subset of the data from the two studies together in Fig. 8. The data from the present study are shown as unconnected symbols, and the data from the Wertheim and van Gelder study are shown as symbols connected by lines. The solid and dashed lines

connect symbols for the same and opposite direction of eye and background motion, respectively. As shown, the pattern of results for the two studies is similar across the range of common background velocities.

Brenner & van den Berg (1994) also found an asymmetry in perceived speed that depended on the relative direction of eye and background motion. Unlike the task in the Wertheim-van Gelder and present studies, the subjects in the Brenner and van den Berg study judged the perceived speed of the pursuit target, not the background motion (display size of $35 \times 22°$). Subjects pursued a target that moved across a textured background. At some point in the presentation, the background velocity could be manipulated and at the same time the target's speed would either increase, decrease, or remain the same. Subjects had to indicate whether the target's speed had changed. The results showed that when the eyes moved in a direction opposite the background motion, pursuit target velocity was perceived to be constant regardless of changes in the velocity of the pursuit target or background, provided the relative motion between the two remained the same. When the eyes moved in the same direction as the background, the pursuit target was perceived to remain the same at a velocity between the constant relative-motion velocity and the initial target velocity. They proposed that when the eyes moved in the same direction as the background motion, perceived speed was influenced by an extraretinal signal that underrepresented eye motion. However, when the eyes and background motion were in opposite directions, the perceived speed of the pursuit target was based on the retinal slip of the background motion. Their results and interpretation are opposite to ours. In our study, with the large display, perceived speed appears little influenced by an extraretinal signal when the eyes move in the same direction as the background. But when the eyes move in the opposite direction to the background, perceived speed appears to be influenced by an extraretinal signal that over-represents eye motion. The difference in results and interpretation between the two studies may be due to the fact that the subjects in our study judged the speed of the background motion and the subjects in the Brenner and van den Berg study judged the speed of the pursuit target. Further studies are needed to determine the reason for the discrepancy.

The results of our study appear to contradict the claim made in other studies that eye movements have little to no effect on the perception of distal stimulus motion (Warren & Hannon, 1990; Royden, Banks & Crowell, 1992; Royden, Crowell & Banks, 1994). These experiments investigated the role of eye movements on the accuracy of heading judgments. The size of the displays used in the these experiments is comparable to our large stimulus display where the subjects underestimated the speed of the distal stimulus during eye movements. The fact that the experimental designs of the heading studies are different from the experimental design of our study may account for the discrepancy. For example, the optic flow patterns used in the heading experiments were composed of motion vectors of various directions and speeds whereas in our experiments the motion vectors were of a uniform speed and direction. The heading experiments also differed from ours in that they examined heading perception which is a direction task unlike the speed-perception task in the present study. Whether or not either of these two methodological differences can account for the differences in results between the studies remains to be seen.

It is interesting to note that the results of another recent study demonstrate that heading perception during eye movements is not always accurate (Freeman, Crowell & Banks, 1996). Subjects perceived an oscillation in the heading direction as they pursued an oscillating target. Using a procedure where subjects canceled the perceived heading oscillation by varying the amplitude and phase of a simulated eye rotation, Freeman, Crowell & Banks determined that the gain of the cancellation signal was from 0.5 to 0.8.

6.3. Functional roles

From an ecological perspective, one may ask why the visual system would respond differently depending on the size of the stimulus and the relative direction of eye movements. Komatsu & Wurtz (1988) have provided a logical neurophysiological argument based on cells in MST. Cells in MST that show a synergistic effect between retinal-image motion and eye movements in the opposite direction could distinguish figure from ground or object motion from self motion. Whereas cells that do not show an effect with a large stimulus display could provide information such as retinal slip that drives the pursuit system.

6.4. Summary

Our results demonstrate that eye movements affect the perceived speed of distal-stimuli. Perceived speed depends on the interaction between the distal stimulus size and the eye velocity relative to the distal stimulus motion. When a person's eyes move in the same direction as a distal stimulus, it appears slower than when the person's eyes are still. When a person's eyes move in the opposite direction to a distal stimulus, its perceived speed depends on its size. For small distal stimuli, eye movements in the opposite direction to the stimulus serve to increase the perceived speed of the stimulus. For large distal stimuli, eye movements in the opposite direction to the stimulus serve to decrease the perceived speed of the stimulus.

Acknowledgements

The authors thank Elisabeth Fine and an anonymous reviewer for helpful comments on an earlier draft and Xinrong Guo for software development. This research was sponsored by the Air Force Office of Scientific Research, Air Force Systems Command, USAF, under grant AFOSR-F49620-94-1-0187 to KAT. The U. S. Government is authorized to reproduce and distribute reprints for Governmental purposes not withstanding any copyright notation thereon. Portions of this work were presented at the Association for Research in Vision and Ophthalmology conference held in Ft. Lauderdale, Florida, May, 1995.

References

Brenner, E., & van den Berg, A. V. (1994). Judging object velocity during smooth pursuit eye movements. *Experimental Brain Research*, *99*, 316–324.

Cornsweet, T. N. (1962). The staircase-method in psychophysics. *American Journal of Psychology*, *75*, 485–491.

Crane, H., & Steele, C. (1985). Generation-V dual-Purkinje-image eyetracker. *Applied Optics*, *24*, 527–537.

Fendick, M. (1985). *The clinical measurement of vernier acuity. Paper presented at the Topical Meeting on Noninvasive Assessment of Visual Function*. Nevada: Incline Village.

Freeman, T. C. A., Crowell, J. A., & Banks, M. S. (1996). Perceived heading during real pursuit eye movements is not always accurate. *Investigative Ophthalmology and Visual Science Suppl.*, *37*, 454.

Gibson, J., Smith, O., Steinschneider, A., & Johnson, C. (1957). The relative accuracy of visual perception of motion during fixation and pursuit. *American Journal of Psychology*, *70*, 64–68.

Komatsu, H., & Wurtz, R. H. (1988). Relation of cortical areas MT and MST to pursuit eye movements. III. Interaction with full-field visual stimulation. *Journal of Neurophysiology*, *60*, 621–644.

Mack, A., & Herman, E. (1973). Position constancy during pursuit eye movements: an investigation of the Filehne illusion. *Quarterly Journal of Experimental Psychology*, *25*, 71–84.

Pola, J., & Wyatt, H. (1989). The perception of target motion during smooth pursuit eye movements in the open-loop condition: characteristics of retinal and extraretinal signals. *Vision Research*, *29*, 471–483.

Royden, C. S., Banks, M. S., & Crowell, J. A. (1992). The perception of heading during eye movements. *Nature*, *360*, 583–585.

Royden, C. S., Crowell, J. A., & Banks, M. S. (1994). Estimating heading during eye movements. *Vision Research*, *34*, 3197–3214.

Turano, K. A., & Heidenreich, S. M. (1996). Speed discrimination of distal stimuli during smooth pursuit eye motion. *Vision Research*, *36*, 3507–3517.

Warren, W. H. J., & Hannon, D. J. (1990). Eye movements and optical flow. *Journal of the Optical Society of America A*, *7*, 160–169.

Watson, A. B., & Turano, K. (1995). The optimal motion stimulus. *Vision Research*, *35*, 325–336.

Wertheim, A. (1987). Retinal and extraretinal information in movement perception: how to invert the Filehne illusion. *Perception*, *16*, 299–308.

Wertheim, A. H. (1981). On the relativity of perceived motion. *Acta Psychologia*, *48*, 97–110.

Wertheim, A. H. (1994). Motion perception during self-motion: the direct versus inferential controversy revisited. *Behavioral and Brain Sciences*, *17*, 293–355.

Wertheim, A. H., & van Gelder, P. (1990). An acceleration illusion caused by underestimation of stimulus velocity during pursuit eye movements: Aubert-Fleischl revisited. *Perception*, *19*, 471–482.

Nonlinear contribution of eye velocity to motion perception

Kathleen A. Turano and Robert W. Massof

The Johns Hopkins University School of Medicine,
Wilmer Eye Institute, Baltimore, MD

Supported by the Air Force Office of Scientific Research, Air Force Materiel Command, USAF, under grant number F49620-97-1-0028. The U.S. Government is authorized to reproduce and distribute reprints for Governmental purposes notwithstanding any copyright notation thereon.

Running head: Nonlinear contribution of eye velocity

Key words: eye movements, smooth pursuit eye movements, motion perception, extra-retinal signal

Please Address Correspondences to:
Kathleen Turano
Lions Vision Center
550 N. Broadway, 6th floor
Baltimore, MD 21205
(410) 502-6434
FAX (410) 955-1829
Email: kathy@lions.med.jhu.edu

Manuscript submitted December 6, 1999 to Vision Research

ABSTRACT

The aim of this study was to test the hypothesis that an extra-retinal signal combines with retinal velocity in a linear manner as described by existing models to determine perceived velocity. To do so, we utilized a method that allowed the determination of the separate contributions of the retinal-velocity and the extra-retinal signals for the perception of stimulus velocity. We determined the velocity (speed and direction) of a stimulus viewed with stationary eyes that was perceptually the same as the velocity of the stimulus viewed with moving eyes. Eye movements were governed by the tracking (or pursuit) of a separate pursuit target. The velocity-matching data were unable to be fit with a model that linearly combined a retinal-velocity signal and an extra-retinal signal. A model that was successful in explaining the data was one that takes the difference between two simple saturating nonlinear functions, g and f, each symmetric about the origin, but one having an interaction term. That is, the function g has two arguments: retinal velocity, $\dot{R}$, and eye velocity, $\dot{E}$. The only argument to f is retinal velocity, $\dot{R}$. Each argument has a scaling parameter. A comparison of the goodness of fits between models demonstrated that the success of the model is the interaction term, i.e. the modification of the compensating eye velocity signal by the retinal velocity prior to combination.

INTRODUCTION

If a person moves his or her eyes to track a moving object in the scene, the retinal image is changed. The smooth pursuit eye movements add a velocity field to the visual scene, changing the speed and/or direction of the motion in the retinal image. Despite retinal image motion from eye movements, we rarely misinterpret the motion to mean there is a moving visual scene.

As early as the nineteenth century, it was hypothesized that retinal image motion from eye movements is discounted by an extra-retinal motion signal, i.e. a neural signal that carries information about the eye movement.[1] The perception of motion was thought to be the difference between a signal reflecting retinal-image motion and the extra-retinal motion signal.[1, 2] The existence of an extra-retinal motion signal has been implicated by observations such as the movement of an afterimage or a stabilized image when it is viewed while moving one's eyes[1, 3] and more recently by a case report[4] of a patient with a cortical lesion. The patient presumably lacked the extra-retinal signal linked to eye movements and as a consequence perceived motion of the stationary background during eye movements.

While it is commonly assumed that an extra-retinal signal exists, observations suggest that the extra-retinal signal does not fully discount (or compensate for) the changes in the retinal image due to eye movements. For example, stationary backgrounds appear to move in the opposite direction of an eye movement—the Filehne illusion, [5] and objects appear to move slower when they are pursued than when they are viewed with stationary eyes—the Aubert-Fleischl phenomenon.[6] Furthermore experimental studies have demonstrated perceptual errors in the speed and direction of moving objects when subjects move their eyes.[7-10] This lack of compensation has been regarded as representing a less-than-unity gain for the extra-retinal signal. According to a modification of the traditional theory,

$$\dot{R} - \varepsilon \dot{E} = \dot{\psi} \qquad \text{Eq. 1}$$

where $\dot{\psi}$ is perceived velocity, $\dot{R}$ is retinal velocity, and $\varepsilon \dot{E}$ is estimated eye velocity. The parameter, ε, is the gain of the extra-retinal signal that relates the actual eye velocity, $\dot{E}$, to the estimated eye velocity*.

Although this model can account for some findings, more recent studies[7-9, 11] challenge this simple modification of the traditional model. For example, the compensation of eye movements for motion perception has been shown to be influenced by the relative direction of the eye movement and stimulus motion,[7, 9, 10] preceding stimuli,[11] and stimulus characteristics. Some of the stimulus characteristics that have been shown to affect the eye-movement compensation are size,[7, 9] retinal eccentricity,[12] duration,[13] and spatial frequency.[8] These studies indicate that the process by which the visual system compensates for changes in the retinal-image motion caused by smooth pursuit eye movements is not as simple as had been previously thought.

Freeman and Banks[8] recently proposed a parameterized model of perceived velocity that consists of an extra-retinal signal that inaccurately estimates eye velocity and a retinal-velocity signal that inaccurately estimates the retinal velocity. The inaccuracies can be viewed as gains of the signals. In the Freeman and Banks study, the stimulus spatial frequency was shown to modify the perceived speed of the stimulus during eye movements. Their model (Equation 2), with a retinal-velocity signal gain that varied with stimulus spatial frequency and an extra-retinal signal gain that remained constant, could explain the data. According to Freeman and Banks,[8]

$$\rho(\Omega)\dot{R} - \varepsilon\dot{E} = \dot{\psi} \qquad \text{Eq. 2}$$

where $\rho(\Omega)\dot{R}$ is the estimated retinal image velocity. The parameter, ρ, is the retinal velocity gain that relates the actual retinal image velocity to the estimated retinal image velocity and is affected by the stimulus's characteristics, Ω.

The aim of this study was to test the hypothesis that an extra-retinal signal is combined with a retinal-velocity signal in a linear manner as described by existing models to determine perceived

* In order to keep the sign convention simple, we specify velocities in the world coordinates. For example, a positive retinal velocity corresponds to the retinal velocity that results from viewing, with stationary eyes, a stimulus that moves to the right. A positive eye velocity corresponds to an eye movement to the right.

velocity. To do so, we needed to determine the separate contributions of the retinal-velocity signal and the extra-retinal signal for the perception of stimulus velocity. Under normal viewing situations, movements of the eye cause the image to move on the retina. Consequently the perceived motion could be the result of the retinal image motion, the extra-retinal signal, or both. To isolate and study the two signals separately, we employed an image stabilization method. This method allowed us to control retinal image motion independent of eye movements. Specifically, the image of the stimulus display was slaved to the subject's eye movements. The image of the display screen moved in synchrony with the eye movement so that its image remained stable on the retina, irrespective of eye velocity. With this technique, we could control the retinal velocity by manipulating the movement of the stimulus on the display.

METHODS

Subjects. Three observers (including the first author) with normal or corrected-to-normal acuities, well trained in the fixate-pursue procedure, served as subjects.

Stimulus-generation and display apparatuses. The stimuli were generated by a Silicon Graphics OCTANE workstation and displayed on a high-resolution CRT monochrome monitor (IKEGAMI 19 in. diagonal, P104 phosphor). The IKEGAMI CRT display is refreshed at a rate of 60 Hz without interlace. Viewing distance was 0.57 meters. The stimulus was an array of randomly positioned dots (density of 1 dot/deg^2) that moved horizontally within a stationary 24° x 24° window. Each dot was composed of a 3 x 3 pixel array (5.4' x 5.4') and had a luminance of 28.5 cd/m^2. A single square (5 x 5 pixel array—9' x 9', 28.5 cd/m^2), positioned within a horizontal gap (2.5°) that divided the window, served as both the stationary fixation point (in the fixate phase) and the pursuit target (in the pursue phase).

Eye movement recording and analysis. Eye velocity was measured using a Generation-V dual Purkinje-image eyetracker.[14] The subject viewed the display with his or her right eye and wore an opaque patch over the left eye. The subject's head was steadied with a bite bar and headrest. Eye velocity was determined from the voltage analogs of horizontal eye position. The voltages were fed into an analog-to-digital converter every 10 ms and stored on a computer for off-line analysis. Voltage was converted to degrees of visual angle, on the basis of each subject's calibration results. The slopes of the eye positions over time were computed separately for the fixation and pursuit intervals of each trial. From these slopes, average eye velocity for the fixation and pursuit intervals was computed. Prior to calculating smooth pursuit eye velocity, saccadic eye movements were identified and eliminated in the manner that we have used in past studies.[9, 15]

Prior to data collection, eye movements were calibrated in the following manner: Twenty-five equally spaced points, extending 6° horizontally and vertically, were displayed in sequence on a CRT display screen positioned 2 meters in front of the subject. To calibrate each position, a dot appeared at the center of the monitor and the subject pushed a button when she or he was fixating the dot. The central dot then disappeared, and a calibration dot appeared. The subject fixated that dot, and the voltage and screen positions were recorded. To convert voltage to degrees of visual angle, a regression line was fit to the dots' horizontal positions, expressed in terms of visual angle, plotted against the horizontal positions of the eye, expressed in terms of voltage.

The retinal velocity of the stimulus was controlled by the stabilization of the stimulus display with a Generation V dual Purkinje image eye tracker. The target for pursuit and fixation was presented on a separate monitor from the one that displayed the stimulus, and the images on the two monitors were superimposed optically (see Figure 1). With this method, the eye movements were monitored by the eyetracker and the signals were sent to the servo-controlled mirrors (designated in the figure as horizontal and vertical deflection mirrors) that rotate in response to the signals to compensate for the subject's eye movements. The image on the stimulus display passed through this optical path with the result that the retinal velocity of the moving

stimulus was unaffected by eye movements. For example, a stimulus moving at 2 °/s had a retinal speed of 2°/s, regardless of the eye velocity. A half-silvered mirror positioned at location A produced another optical path. Images from a separate display monitor that pass through this optical path bypass the optical path used for stabilization. We present a target that is used for pursuit and fixation on this second display with the result that its retinal image undergoes changes consistent with a person's eye movements. The images (stimulus and pursuit/fixation target) on the two monitors were superimposed optically.

We used the after-image technique described by Kelly,[16] to achieve optimal stabilization. An initial gain setting of the eyetracker signal was established by having the subject alternately fixate between two unstabilized marks as he or she adjusted the potentiometer to make a stabilized dot move from one unstabilized mark to the other. After the initial gain setting was made, a finer gain setting was achieved by having the subject view a stabilized bright line as the subject moved his or her eyes back and forth. The gain of the eyetracker signal was adjusted so that the dark afterimage was positioned behind the bright line and hence could not be seen. Using these methods, the average error in repeating the optimal gain setting was 0.6%.

Figure 1 about here

Procedure. Velocity matches were made in a two-step process. The first step consisted of establishing a direction match, and the second step consisted of obtaining velocity matches to the stimuli whose directions were perceptually matched. For both direction matching and velocity matching, on each trial a moving stimulus was presented twice in succession (shown in Figure 2 as translating dots). In the first interval, the stimulus moved at a test velocity. During this interval, the subject fixated a stationary spot. In the second interval, the stimulus moved at a base velocity, and the subject tracked the pursuit target (a spot translating across the screen). To establish direction matches, after each trial, the subject adjusted the direction of the stimulus (left or right) in the first interval to match the direction of the stimulus in the second interval. Upon completion of the direction-matching step, speed matches were made using the direction-matched stimuli. To obtain speed matches, for each trial, the subject indicated whether the test speed, a pre-determined base

speed ± a delta speed, was faster or slower than the base speed in the second interval. On the next trial, the test speed was decreased or increased depending on the subject's response on the previous trial. This process continued until the subject reported that the two speeds were equal. At the point of perceptual equivalence, the test speed defined the speed match threshold. No feedback was given. (For the conditions that we tested, the directions were reported perceptually matched at the end of testing, when the subjects reported that the speeds were matched.)

Figure 2 about here

In order to manipulate eye velocity in the experiment, a small square was optically superimposed on the stimulus. Subjects were instructed to keep their eyes fixed on the square that either remained stationary in the center of the display or moved across the screen. The image of the square passed through a separate optical path from the stimulus display, and it was not yoked to the subject's eye movements.

With this procedure, we are able to determine the separate contributions of the retinal-velocity signal and the extra-retinal signal for the perception of motion. In the first interval, the subject viewed the stimulus with stationary eyes so that the eye velocity was approximately 0. Perceived velocity of the stimulus in this interval had to be derived solely from the retinal velocity. In the second interval, perceived velocity of the reference stimulus was derived from the extra-retinal signal generated from the pursuit eye movement and a constant retinal velocity from the reference stimulus. (Because the retinal velocity of the stimulus was unchanged by the pursuit eye movements with this method, we were able to hold the retinal velocity constant.) At perceptual equivalence the retinal-velocity signal from the test stimulus produced the same velocity perception as the combined extra-retinal signal and the retinal-velocity signal. By systematically varying eye velocity across a range of base velocities, we were able to map out the contributions of the two velocity signals for compensation. In the special case where the base velocity was 0°/s, the velocity of the test stimulus at perceptual equivalence revealed the retinal velocity that is perceived to be equivalent to the extra-retinal signal.

Experiment 1: Velocity matches for a stimulus velocity of 0°/s

To obtain direct evidence of the existence of an extra-retinal visual motion signal and to determine how the illusory motion that it generates relates to eye velocity, we measured velocity match thresholds for a base velocity of 0°/s for a range of eye velocities. Since the eyes were stationary during the first interval, no extra-retinal signal was generated and therefore the perception of motion had to be due to the retinal image motion. In the second interval, there was no retinal-image motion. Therefore any perception of motion during the second presentation had to arise from the extra-retinal signal. At perceptual equivalence, the retinal image velocity that produced the same motion percept as the extra-retinal signal was determined.

Results: Experiment 1.

Subjects observed that when the stationary stimulus was viewed with stationary eyes the stimulus appeared stationary. However, when the stationary stimulus was viewed while the eyes were moving, the stationary stimulus appeared to move with the eyes. Because the image of the stimulus display was slaved to the subject's eye movements and the stimulus was stationary on the display, there was no retinal image motion. The perceived illusory motion of the stimulus must be due to an extra-retinal signal that is associated with the movement of the eyes.

Subjects made perceptual matches across a range of eye velocities. Figure 3 is a graph of the retinal velocity of a test stimulus perceived to be equal to a stationary reference stimulus viewed with moving eyes. As shown, the stationary stimulus was perceived to be moving in the same direction as the smooth pursuit eye movement, corroborating the subjective impressions. This illusory motion is the consequence of the compensation process. Because the retinal velocity of the stationary stimulus was 0°/s, the speed match threshold reflected the retinal velocity equivalence of the extra-retinal signal.

The data show that the magnitude of the speed match threshold increased with increasing eye velocity for both leftward (shown as negative eye velocity) and rightward (positive eye velocity) eye movements. The data would fall on the identity line in Figure 3 if perceived velocity of motion appeared matched when retinal image velocity equaled eye velocity. The matches deviate

from the line (with slopes of 0.84, 0.82, and 0.74 for subjects smh, kat, and fjt, respectively). These results indicate that the extra-retinal signal underestimated eye velocity—corroborating earlier impressions.[6, 8, 17-20] This conclusion implies that the perceived illusory motion of the stationary world during a smooth pursuit eye movement would be equivalent to that produced by an 80% reduction in actual retinal image motion (if the signals add). A comparison of the motion percepts generated from eye movements and from retinal image motion indicates that the eye has to move at a speed approximately 1.25 times that of the retinal image motion to produce equivalent motion percepts.

Figure 3 about here

Experiment 2: Velocity matches for stimulus velocities of 2°/s and 4°/s

The results of Experiment 1 demonstrated that smooth pursuit eye movements generate an internal motion signal, i.e. an extra-retinal signal, that is in the same direction as the eye movement and is indistinguishable from a motion percept generated from retinal image motion. In this experiment we examined how the extra-retinal and retinal velocity signals combine. Velocity match thresholds were determined for base speeds of 2°/s and 4°/s. In these conditions the perception of motion of the dots in the second interval is the result of the combination of the base velocity (2°/s or 4 °/s) and an extra-retinal signal.

Results: Experiment 2.

The center and bottom rows of Figure 4 show the graphs of the velocity match thresholds for base velocities of 2°/s and 4°/s, respectively. The three subjects' data are shown in separate columns.The retinal velocities of a test stimulus perceived to be equal to the reference stimulus viewed with moving eyes are plotted against eye velocity. Negative and positive values of eye velocity indicate eye movements in the opposite and same direction to the stimulus. As shown, the data appear to flatten out for eye movements in the same direction as the stimulus (positive values of eye velocity).

Figure 4 about here

Fit of Linear Models

To determine how well the modified traditional model, $\dot{R} - \varepsilon\dot{E} = \dot{\psi}$, fit the data we performed a least squares fit. Using the statistical software program, JMP (SAS Institute, Cary, NC), we estimated the best value for ε, the gain factor of the extra-retinal signal. The model was fit to the combined dataset of the three subjects and three R_{BASE} velocities (0°/s, 2°/s, and 4°/s). The best fitting value for ε was -0.676 (see Table 1). The leftmost graphs in Figure 5 show the three subjects' data with the linear model fits. The top, center, and bottom rows show the data for base velocities of 0°/s, 2°/s, and 4°/s, respectively. As shown, the model fails to account for the data of the fast eye movements.

Table 1 and Figure 5 about here

We then determined whether or not a parameterized linear model, similar to the model proposed by Freeman and Banks,[8] could account for the data. The parameterized linear model, $(\rho)\dot{R} - \varepsilon\dot{E} = \dot{\psi}$, states that perceived velocity is the difference between the estimated retinal velocity signal and the estimated eye velocity signal. The parameter, ρ, is a gain factor that relates the estimated retinal velocity to the actual retinal velocity, and ε is a gain factor that relates the estimated eye velocity to the actual eye velocity. Giving the model a liberal interpretation, we applied the model separately to each of the R_{BASE} velocity datasets (0°/s, 2°/s, and 4°/s). We used JMP to perform a least squares fit to estimate the ratio ε/ρ. The best fitting ratios are shown in Table 1. These ad hoc model fits are shown as solid lines in the center left graphs of Figure 5 (under "Parameterized Linear Model"). The ad hoc parameterized linear model provides a good fit to the 0°/s base velocity data (top graph). However the model does less well in fitting the 2°/s (middle graph) and the 4°/s base velocity data (bottom graph), particularly for fast eye movements in the opposite direction.

Fit of Nonlinear Models

The observation that the linear models failed to fit the data at the fast eye speeds led us to look at simple nonlinear models for eye-movement compensation that incorporate saturating functions. We defined a nonlinear form of the traditional model as

$$f(\dot{R}) - g(\dot{E}) = \dot{\psi}, \qquad \text{Eq. 3}$$

where perceived velocity was the difference between a nonlinear function, g, that related estimated eye velocity to actual eye velocity and a nonlinear function, f, that related estimated retinal velocity to actual retinal velocity. Assuming that f() and g() are approximately linear over some range, but are limited to asymptotic values at extreme velocities, we first evaluated the functions

$$f[\dot{R}] = R_{max}\left(\frac{1}{1+e^{-\rho\dot{R}}} - 0.5\right) \qquad \textit{and} \qquad g[\dot{E}] = R'_{max}\left(\frac{1}{1+e^{-\varepsilon\dot{E}}} - 0.5\right) \qquad \text{Eqs. 4 \& 5}$$

which are linear near zero velocity, and asymptote at $R_{max}/2$ or $R'_{max}/2$ at extreme positive or negative velocities. The gain factors, ρ and ε, control the slopes of the linear portions of the functions.

We determined the values for the three free parameters (ε, ρ, and R_{max}/R'_{max}) using a least squares fit to the combined dataset. The best fitting parameter values are listed in Table 1, and the model fits are shown as solid lines in the center right graphs of Figure 5. As shown, this simple nonlinear model provides a poor fit to the data.

If we superimpose the velocity matches for the three base velocities (0°/s, 2°/s, and 4°/s) on a single graph (Fig. 6), we can observe both a vertical shift in the data and a horizontal shift that is dependent on $\dot{R}_{BASE}$. Motivated by the apparent horizontal shift in the data, we modified the simple nonlinear model to incorporate an interaction term into the compensation signal (Fig. 7). Function g, representing the compensating signal, was modified to receive two inputs: retinal velocity, $\dot{R}$, and eye velocity, $\dot{E}$. The modified function, $g[\dot{E}, \dot{R}]$, is specified as

$$g[\dot{E},\dot{R}] = R'_{max}\left(\frac{1}{1+e^{-\varepsilon\dot{E}-\alpha\dot{R}}} - 0.5\right). \qquad \text{Eq. 6}$$

Figures 6 and 7 about here

We determined the values for the four free parameters (ε, ρ, R_{max}/R'_{max}, and α) using a least squares fit to the combined dataset. The parameter values are listed in Table 1, and the model fits are shown as solid lines in the rightmost graphs of Figure 5. As shown in the graphs, the model provides a good fit to the data of all three base velocities, despite the fact that the model was applied to the combined dataset.

One estimate of a model's goodness of fit is the root mean square error (RMSE) of a model's prediction of the data. The RMSEs for the linear and nonlinear models are shown in Table 1. The ad hoc parameterized linear model (with three free parameters) shows a better fit to the data, which has a RMSE of 0.62, compared to the modified traditional linear model (with one free parameter), which has a RMSE of 0.69. The simple nonlinear model, which also has three free parameters has a high RMSE, 0.97, reflecting its poor fit to the data. The model that best fits the data is the simple nonlinear model with the interaction term (four free parameters). This model has a RMSE of 0.45. The difference between the fits of the two nonlinear models and the ad hoc parameterized linear model demonstrates the importance of the interaction term, i.e. the retinal velocity in the compensation signal to determine perceived velocity. Simply adding degrees of freedom with the nonlinearity is not sufficient to describe the trends in the data.

Discussion

The results of Experiment 1 provided direct evidence for the existence of an extra-retinal signal that is generated by pursuit eye movements. With a stationary stimulus whose retinal image was slaved to the subject's eye movements we were able to isolate the motion percept that was generated by an extra-retinal motion signal during pursuit eye movements. We demonstrated that the motion percept is in the same direction as the eye movement and is indistinguishable from a

motion percept that is generated from retinal image motion. A comparison of the motion percepts generated from eye movements and from retinal image motion indicates that the eye has to move at a speed approximately 1.25 times that of the retinal image motion to produce equivalent motion percepts.

In Experiment 2 we tested the hypothesis that an extra-retinal signal combines with retinal velocity in a linear manner as described by existing models to determine perceived velocity. The results showed that the linear models cannot explain the present data. Linear models, such as the modified traditional model or even an ad hoc parameterized linear model, failed to fit the data, suggesting the existence of nonlinearities, particularly for fast eye speeds.

A model that was successful in explaining the data was one that takes the difference between two simple saturating nonlinear functions, g and f, each symmetric about the origin, but one having an interaction term. That is, the function g has two arguments: retinal velocity, $\dot{R}$, and eye velocity, $\dot{E}$. The only argument to f is retinal velocity, $\dot{R}$. Each argument has a scaling parameter. The difference in goodness of fits between the two nonlinear models demonstrates that the success of the model is the interaction term, i.e. the modification of the compensating eye velocity signal by the retinal velocity prior to combination.

In our model the compensating signal, g [E,R], contains a visual (retinal) component in addition to an eye-velocity component. In this sense our model is similar to the one proposed by Wertheim[21]. In Wertheim's model the reference signal is a combination of visual, extra-retinal, and vestibular signals. In our experiments the head was steadied with a bitebar and headrest maintaining constant vestibular signals throughout the experiment. Therefore the issue of a vestibular input to the compensating signal was not addressed in our model. The two models do differ with respect to the functions relating estimates of eye and retinal velocities and their actual values. In the Wertheim model the estimators were related to the actual values by a scalar, whereas in our model the functions are saturating nonlinearities.

In summary, using a perceptual matching paradigm and a stabilized stimulus display, we have demonstrated that an extra-retinal signal does exist but it does not combine in a linear manner

with retinal velocity to determine perceived velocity. To fit the data it is necessary to introduce saturating nonlinear functions and a retinal-velocity input to the compensating signal to determine perceived velocity.

Figure Legends

Figure 1. An illustration (adapted from[14]) of the modified image-stabilizing system of the Generation V dual Purkinje image eye tracker. Eye movements are monitored by the eyetracker and the signals are sent to the servo-controlled mirrors (designated in the figure as horizontal and vertical deflection mirrors) that rotate in response to the signals to compensate for the subject's eye movements. A half-silvered mirror is positioned at location A in order to produce another optical path in which stimuli presented on a separate display monitor could pass through, bypassing the optical path used for stabilization.

Figure 2. Schematic of procedure. Subjects matched the velocities of two sets of dots (labeled as A and B in figure) randomly positioned within a stationary window. While viewing the first set of dots the subject kept his or her eyes fixed on a small centrally located stationary square. While viewing the second set of dots, the subject pursued the square as it translated across the screen. After the presentation of the two sets of dots, the subject indicated whether the dots in A moved faster or slower than the dots in B. Depending on the subject's response, on the next trial the speed of the dots in A was decreased or increased. This process continued until the subject reported that the two velocities were equal. Time course for each trial is shown at the top.

Figure 3. Velocity match thresholds for a stationary (0°/s) base velocity. The retinal image velocity that perceptually matches the stationary dots viewed during smooth pursuit eye movements. Each data point is the mean of 3 determinations. Error bars represent ±1 SD. Negative and positive eye velocities indicate leftward and rightward eye movements, respectively. Line represents a perfect match between retinal image velocity and eye velocity. Data are for subjects smh (filled circles), kat (squares), and fjt (open circles).

Figure 4. Velocity-match thresholds for base velocities of 0°/s (top), 2°/s (center), and 4°/s (bottom). The retinal image velocity that perceptually matches the reference stimulus viewed during

smooth pursuit eye movements. Negative and positive eye velocities indicate eye movements in the opposite and same direction as the stimulus, respectively. Data for subject smh, kat, and fjt are in the left, center, and right columns, respectively.

Figure 5. Velocity-match thresholds for base velocities of 0°/s (top), 2°/s (center), and 4°/s (bottom). The retinal image velocity that perceptually matches the reference stimulus viewed during smooth pursuit eye movements. Negative and positive eye velocities indicate eye movements in the opposite and same direction as the stimulus, respectively. Lines represent model fits to the data. Column headings indicate the respective models. Data are from three subjects.

Figure 6. Velocity-match thresholds for base velocities of 0°/s (filled squares), 2°/s (open triangles), and 4°/s (filled circles). The retinal image velocity that perceptually matches the reference stimulus viewed during smooth pursuit eye movements. Negative and positive eye velocities indicate eye movements in the opposite and same direction as the stimulus, respectively. Data are from 3 subjects.

Figure 7. A schematic of the present nonlinear compensation model. Perceived velocity, $\dot{\psi}$, is the difference between $f[\dot{R}]$, a saturating nonlinear function relating estimated retinal velocity to actual retinal velocity, and $g[\dot{E}, \dot{R}]$, a saturating nonlinear function estimating the compensating signal from the inputs, retinal velocity ($\dot{R}$) and eye velocity ($\dot{E}$).

References

1. von Helmholtz H. *Treatise on physiological optics*.New York: Dover, 1962; vol III (trans. from the 3rd German ed., JPC Southall)).

2. von Holst E. Relations between the central nervous system and the peripheral organs. *Br J Animal Behav* 1954;2:89-94.

3. Mack A, Bachant J. Perceived movement of the afterimage during eye movements. *Percept Psychophys* 1969;*6*:379-384.

4. Haarmeier T, Thier P, Repnow M, Petersen D. False perception of motion in a patient who cannot compensate for eye movements. *Nature* 1997;*389*:849-852.

5. Filehne W. Uber das optische Wahrnehmen von Bewegungen. *Z. Sinnesphysiol.* 1922;*53*:134-145.

6. Fleischl E. Physiologische-optische notizen. *SB Akad. Wiss. Wien* 1882;*86*:17-25.

7. Wertheim AH, Van Gelder P. An acceleration illusion caused by underestimation of stimulus velocity during pursuit eye movements: Aubert-Fleischl revisited. *Perception* 1990;*19*:471-482.

8. Freeman TCA, Banks MS. Perceived head-centric speed is affected by both extra-retinal and retinal errors. *Vision Res* 1998;*38*:941-946.

9. Turano KA, Heidenreich SM. Eye movements affect the perceived speed of visual motion. *Vision Res* 1999;*39*:1177-1187.

10. Brenner E, van den Berg AV. Judging object velocity during smooth pursuit eye movements. *Exp Brain Res* 1994;*99*:316-324.

11. Haarmeier T, Thier P. Modification of the Filehne illusion by conditioning visual stimuli. *Vision Res* 1996;*36*:741-750.

12. Turano KA, Heidenreich SM. Stimulus size influences the effect of eye movements on perceived speed. *Optical Society Technical Program* 1998;:111.

13. Ehrenstein WH, Mateeff S, Hohnsbein J. Influence of exposure duration on the strength of the Filehne illusion. *Perception* 1987;*16*:253.

14. Crane HD, Steele CM. Generation-V dual-Purkinje-image eyetracker. *Appl Opt* 1985;*24*:527-537.

15. Turano KA, Heidenreich SM. Speed discrimination of distal stimuli during smooth pursuit eye motion. *Vision Res* 1996;*36*:3507-3517.

16. Kelly DH. Motion and vision. I. Stabilized images of stationary gratings. *J Opt Soc Am* 1979;*69* :1266-1274 .

17. Brown JF. The visual perception of velocity. *Psychol Forsch* 1931;*14*:199-232.

18. Mack A, Herman E. A new illusion: the underestimation of distance during pursuit eye movements. *Percept Psychophys* 1972;*12*:471-473.

19. de Graaf B, Wertheim AH. The perception of object motion during smooth pursuit eye movements: adjacency is not a factor contributing to the Filehne illusion. *Vision Res* 1988;*28*:497-502.

20. Wertheim AH. Retinal and extraretinal information in movement perception: how to invert the Filehne illusion. *Perception* 1987;*16*:299-308.

21. Wertheim AH. Motion perception during self-motion: the direct versus inferential controversy revisited. *Behav Brain Sci* 1994;*17*:293-355.

Table 1. Parameter values and goodness-of-fit estimates for th elinear and nonlinear models.

	LINEAR MODEL	AD HOC PARAMETERIZED LINEAR MODEL			SATURATING NONLINEAR MODEL	PRESENT MODEL
PARAMETERS		0°/s	2°/s	4°/s		
ρ	-	-1.259	-1.451	-1.767	0.406	0.235
ε	-0.676	1	1	1	0.351	0.761
h	-	-	-	-	0.648	1.660
α	-	-	-	-	-	0.769
RMSE	0.69	0.62			0.97	0.45

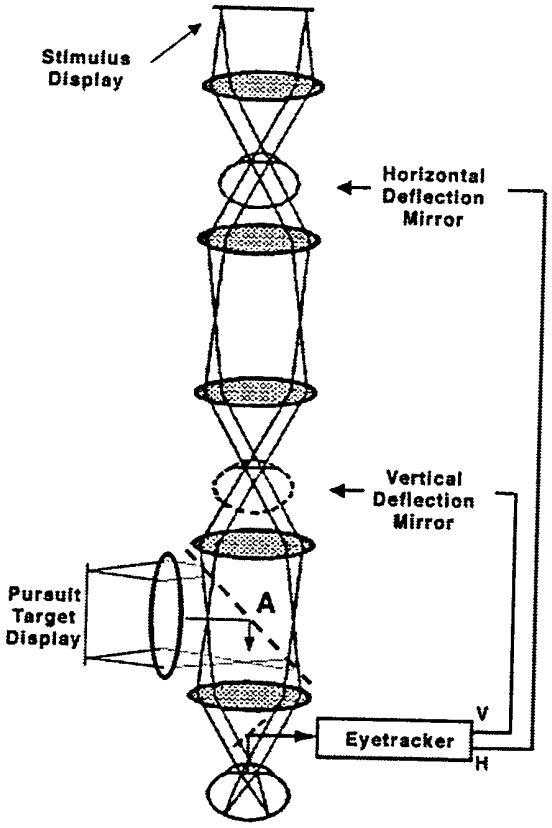
Stimulus
Display
Horizontal
Deflection
Mirror
Vertical
Deflection
Mirror
Pursuit
Target
Display
A
V
Eyetracker
H

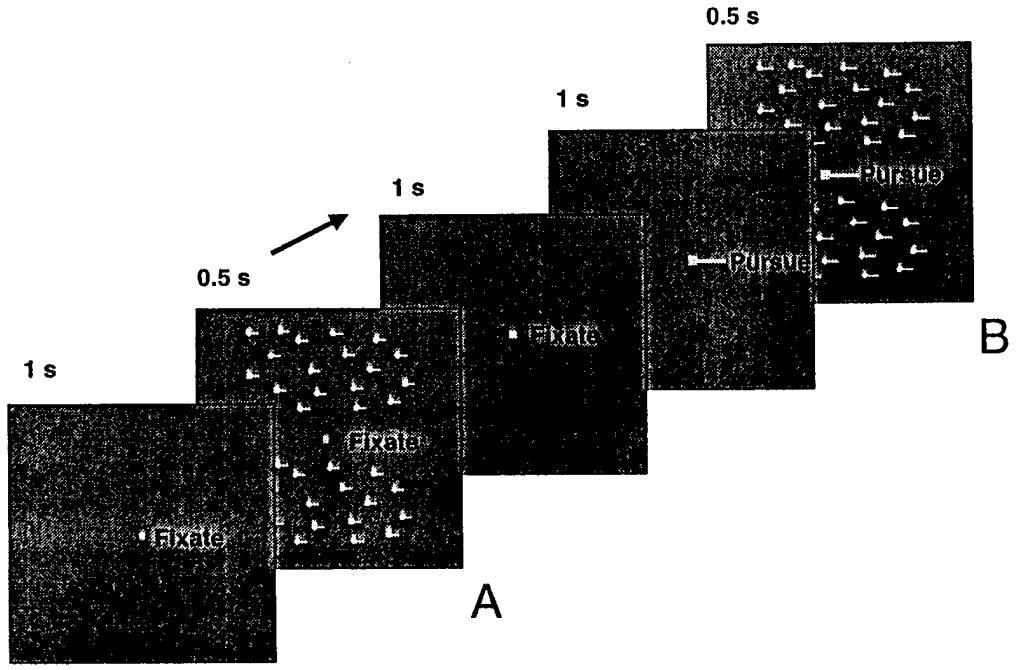
1 s
Fixate
0.5 s
Fixate
1 s
Fixate
A
1 s
Pursue
0.5 s
Pursue
B

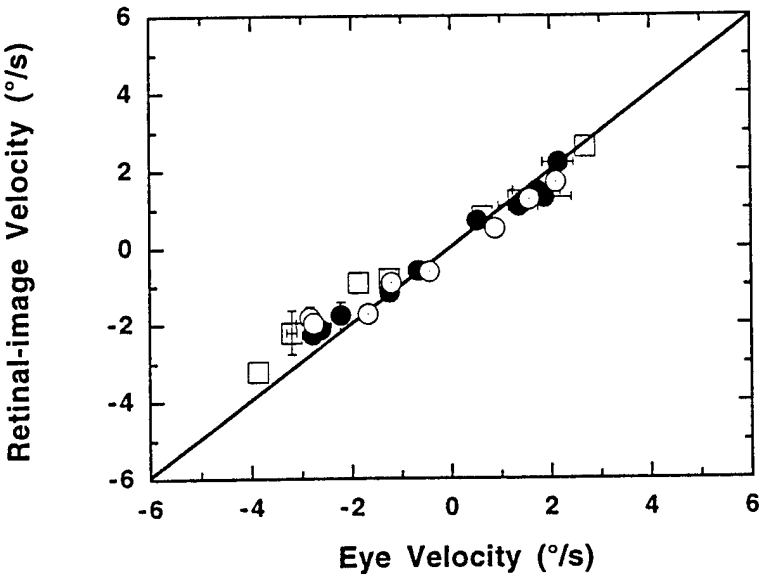
Retinal-image Velocity (°/s)
6
4
2
0
-2
-4
-6
-6
-4
-2
0
2
4
6
Eye Velocity (°/s)

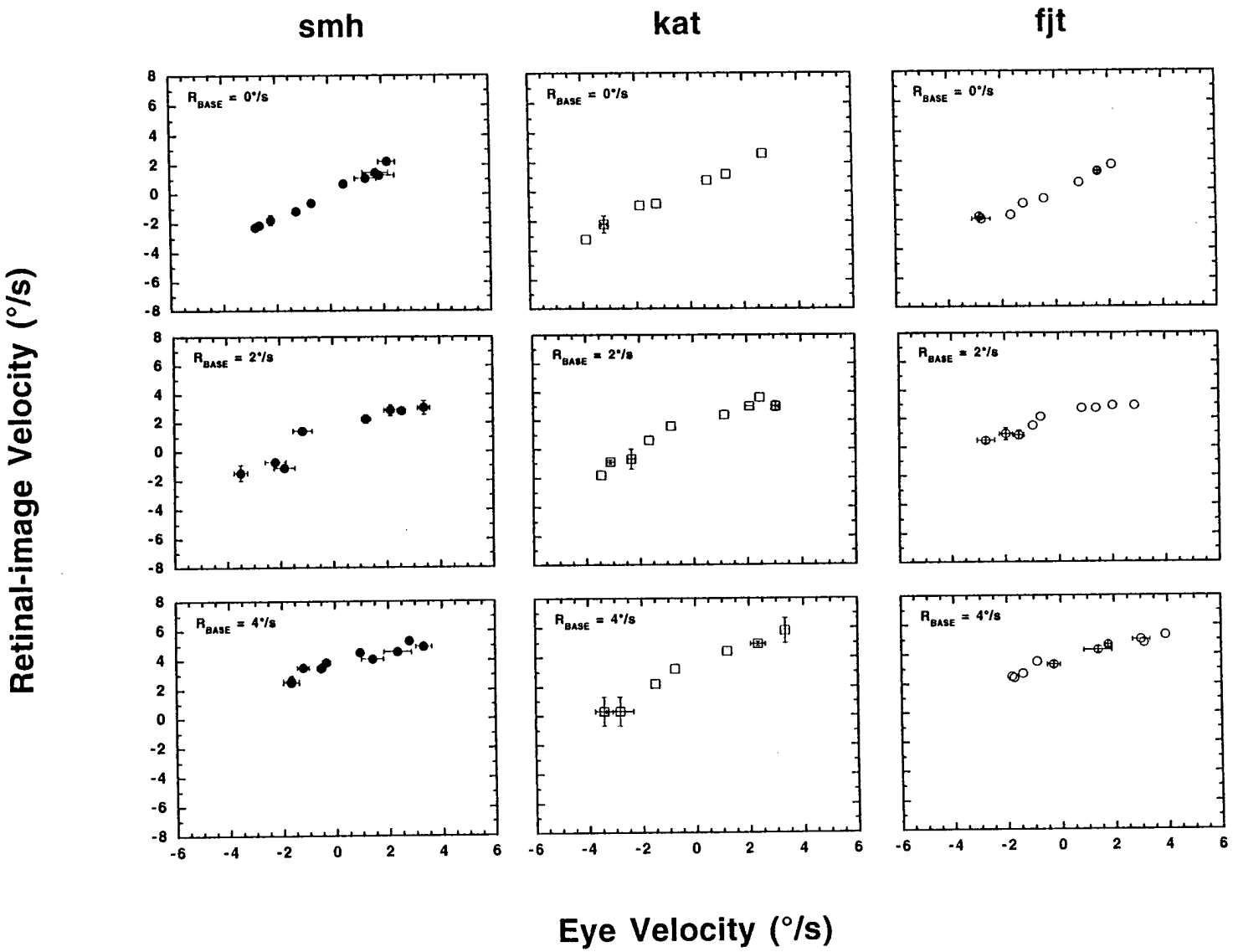
smh
kat
fjt
R_BASE = 0°/s
R_BASE = 2°/s
R_BASE = 4°/s
Retinal-image Velocity (°/s)
Eye Velocity (°/s)
8
6
4
2
0
-2
-4
-6
-8
-6
-4
-2
0
2
4
6

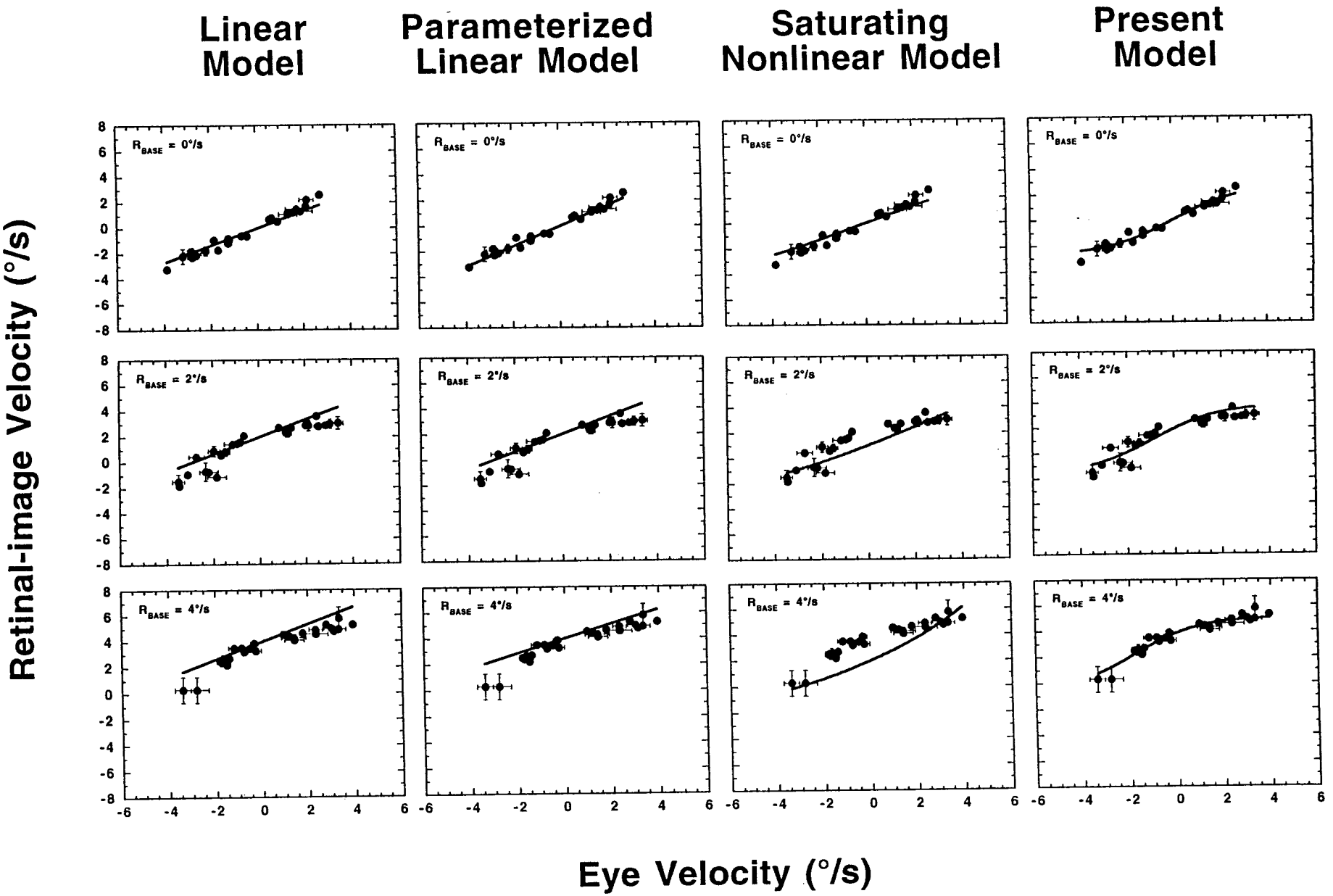
Linear Model
Parameterized Linear Model
Saturating Nonlinear Model
Present Model
Retinal-image Velocity (°/s)
Eye Velocity (°/s)
R_BASE = 0°/s
R_BASE = 2°/s
R_BASE = 4°/s

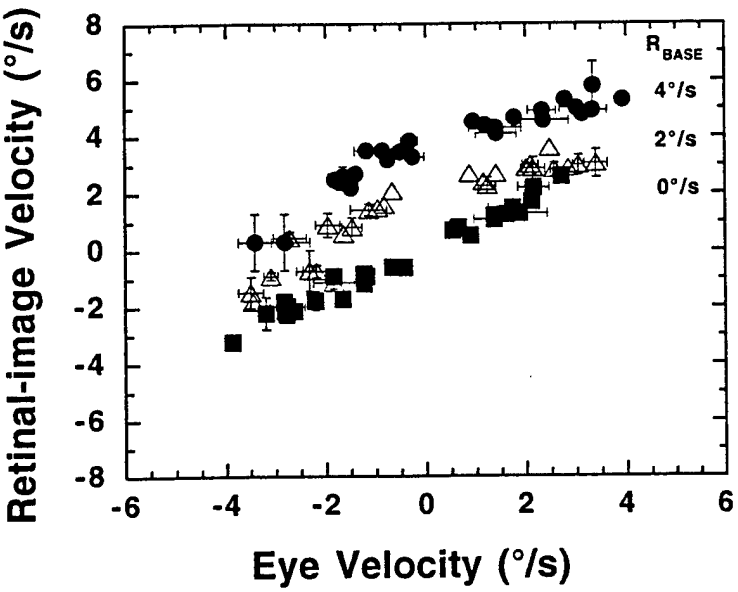
Retinal-image Velocity (°/s)
8
6
4
2
0
-2
-4
-6
-8
-6
-4
-2
0
2
4
6
Eye Velocity (°/s)
R BASE
4°/s
2°/s
0°/s

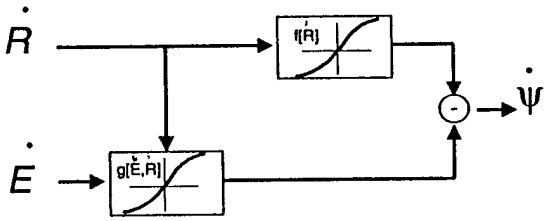

$$g[\dot{E},\dot{R}] = R'_{max} \frac{1}{(1+e^{-\varepsilon E-\alpha R} - 0.5)}$$

$$f[\dot{R}] = R_{max} \frac{1}{(1+e^{-\rho R} - 0.5)}$$